Extrinsic Stellar Variability

The Variable Universe – Lecture 03
Fall Semester 2022

Richard Anderson
richard.anderson@epfl.ch
022 379 24 25
Sauverny Observatory #265

EPFL

Questions from last week?

Hertzsprung-Russell Diagram (HRD)

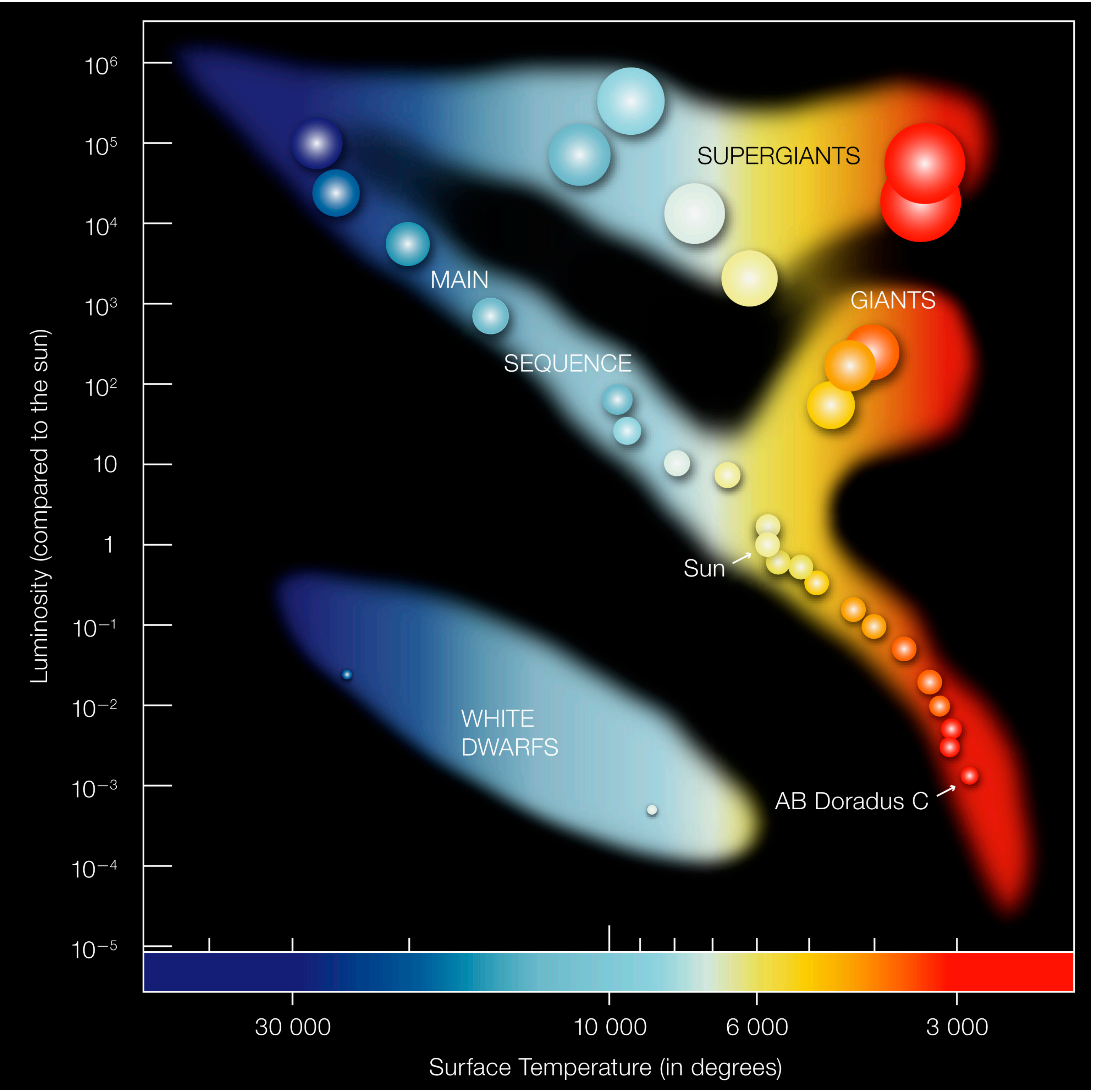

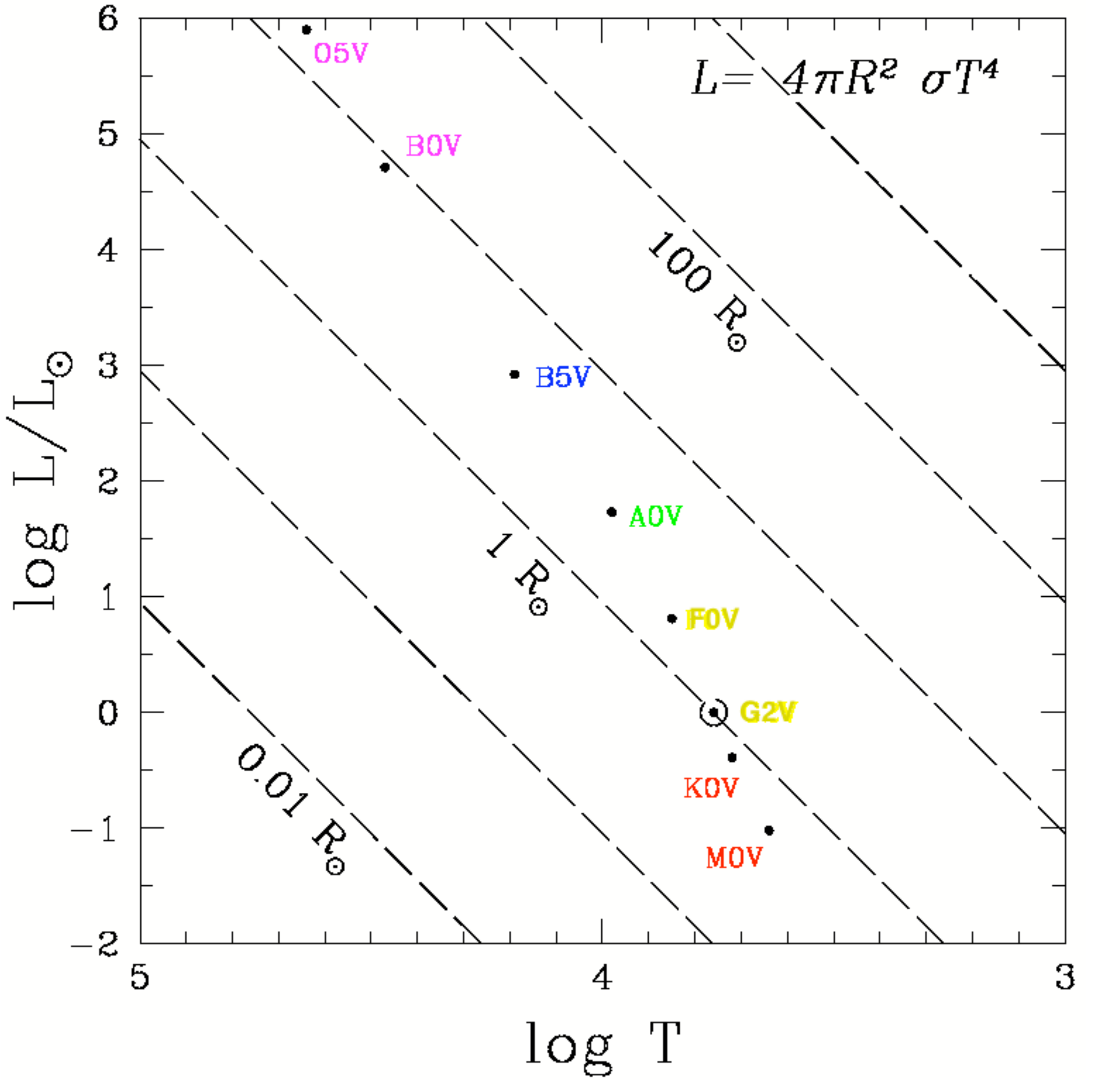

Color-Magnitude Diagram (CMD)

- $m = -2.5 \log_{10}\left(\frac{f_{obs}}{f_{std}}\right)$
- $m_a - m_b \propto \log(\mathrm{T_{eff}})$
- $M - m = 5 \log\left(\frac{d}{10\ \mathrm{pc}}\right) - 5\ + A$
- $L = 4\,\pi\,\sigma\,R^2\,T_{\mathrm{eff}}^4$
- $L = 10^{-0.4M_{\mathrm{bol}}} \cdot 3.0128 \times 10^{28}\ \mathrm{W}$
- $M_{\mathrm{bol}} - M_{bol,\odot} = -2.5 \log\left(\frac{L}{L_\odot}\right)$

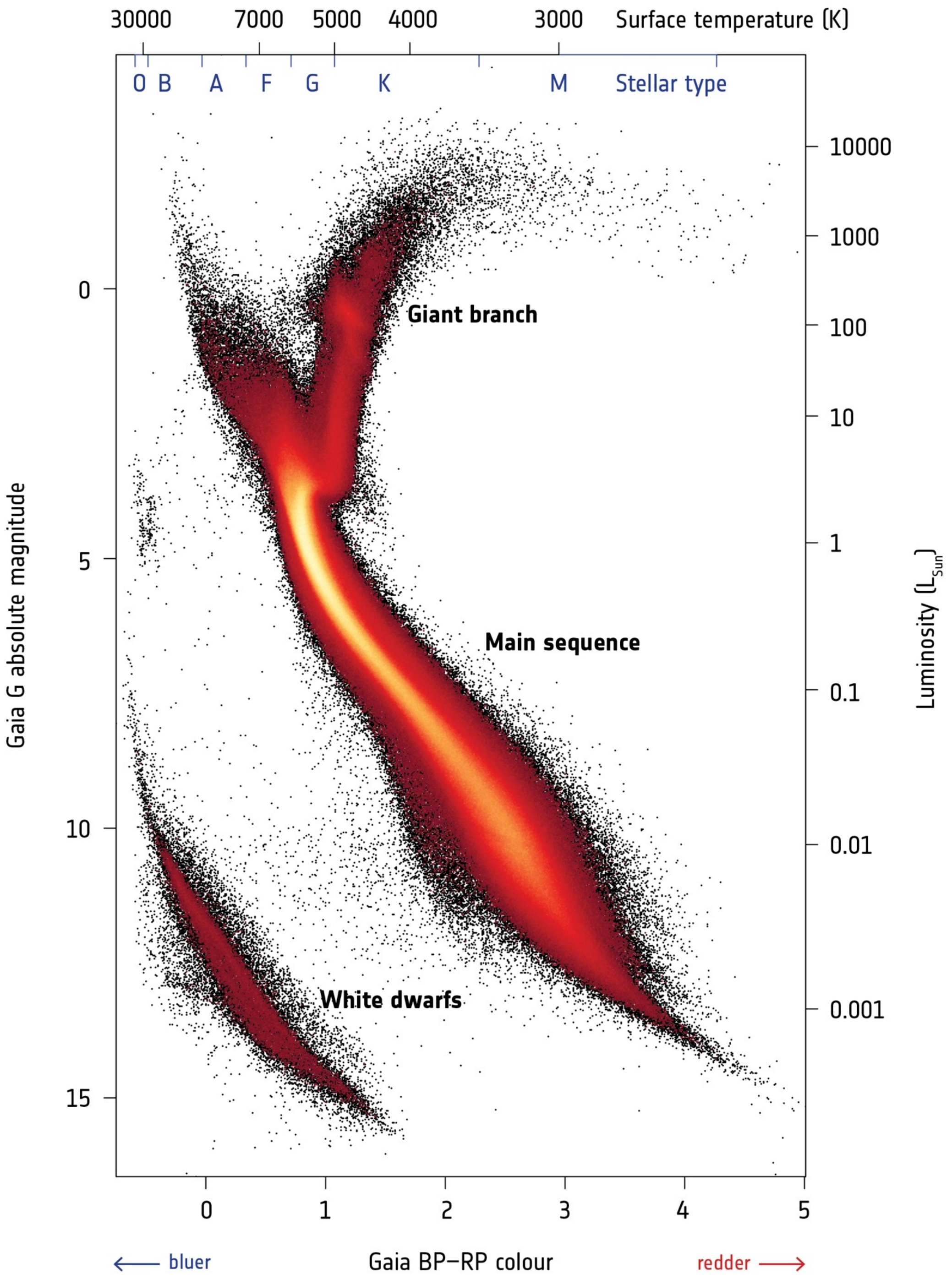

Quantifying variability

- Magnitudes are logarithmic scale
- Brighter : smaller numerical value!
- 5 magnitude = 100x flux
- 1% flux difference: $\Delta m \approx 0.01$ mag
- What is maximum Δm in eclipsing binary star system?
- Double the flux: $\Delta m \approx -0.75$ mag

$$m = -2.5 \log_{10} \left(\frac{f_{obs}}{f_{std}} \right)$$

$$\Delta m(t) = -2.5 \log_{10} \left(\frac{f(t)}{f(t_{\mathrm{ref}})} \right)$$

Photometric

Six extra dimensions from
- Astrometry
- Spectroscopy

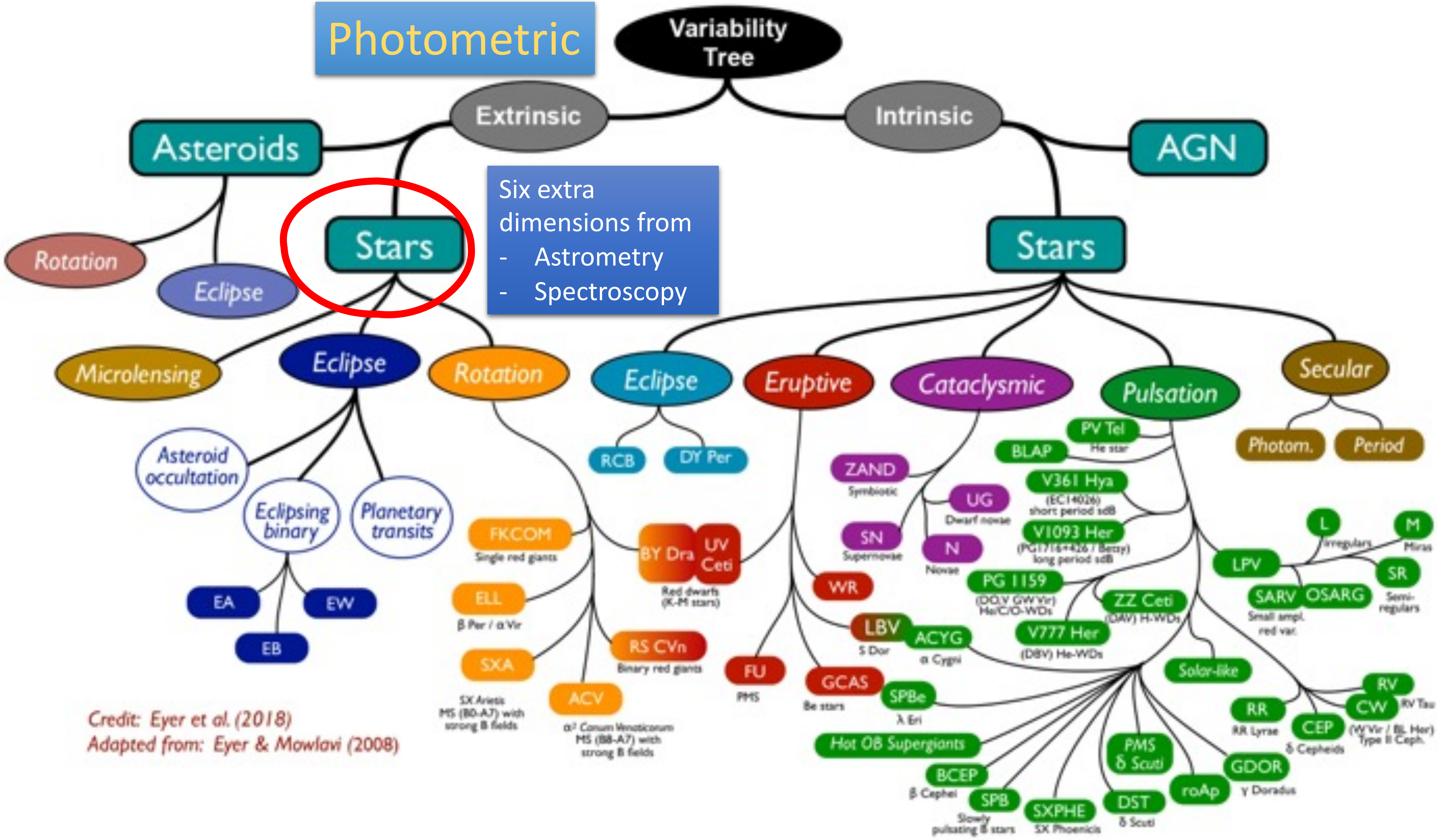

Extrinsic variable stars

are those in which the light output varies either due to processes external to the star itself or due to the rotation of the star

Part I : multiple star systems

Why study stellar multiplicity

- How many stars are there?
- Mass
- Distance
- How do stars evolve?

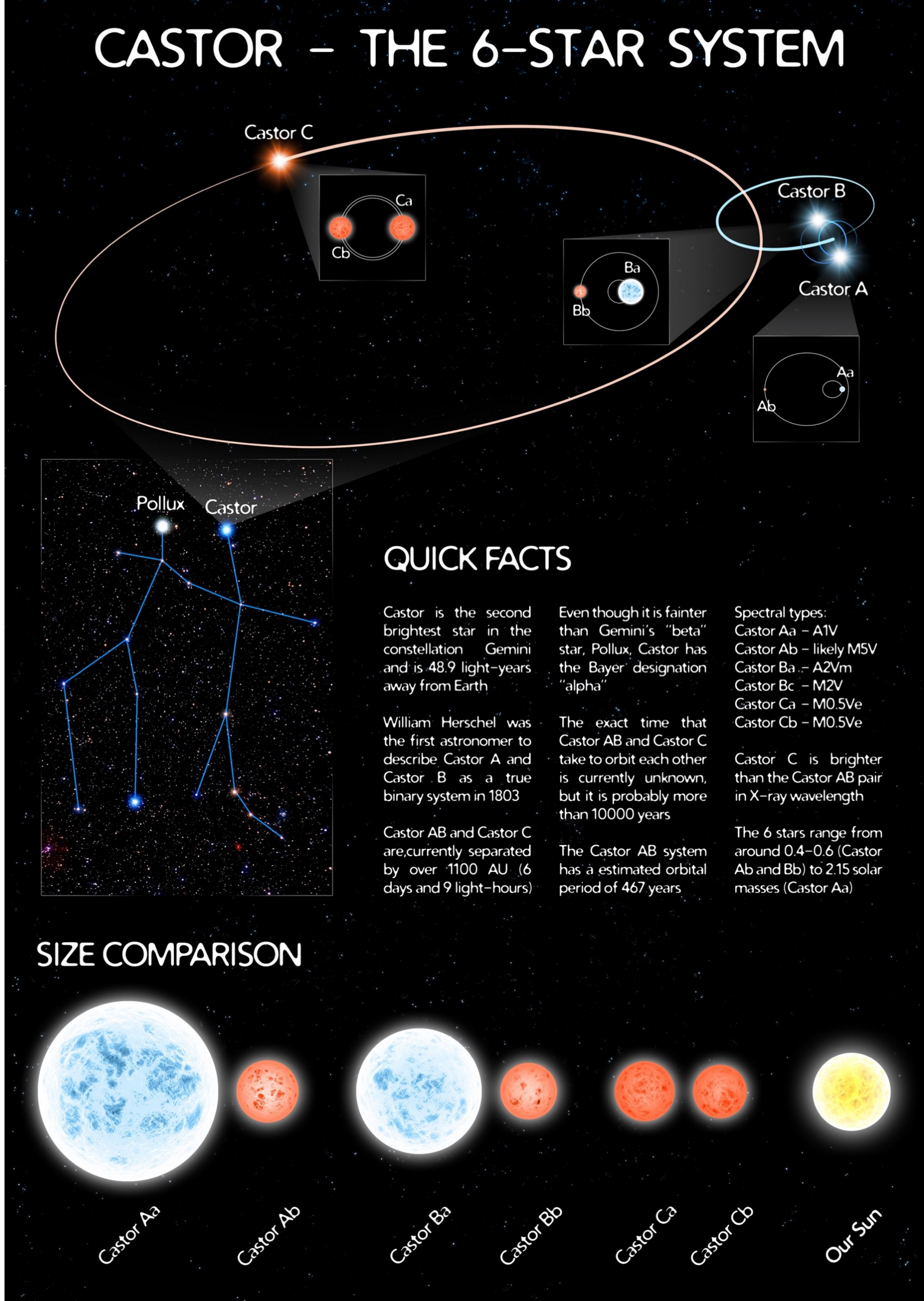

Multiple star systems

Located within 25pc (RECONS, 2014)

- **1533** single star systems,
- **509** binary systems,
- **102** triple systems,
- **19** quadruple systems,
- **4** quintuple systems, and even
- **1** sextuple system.

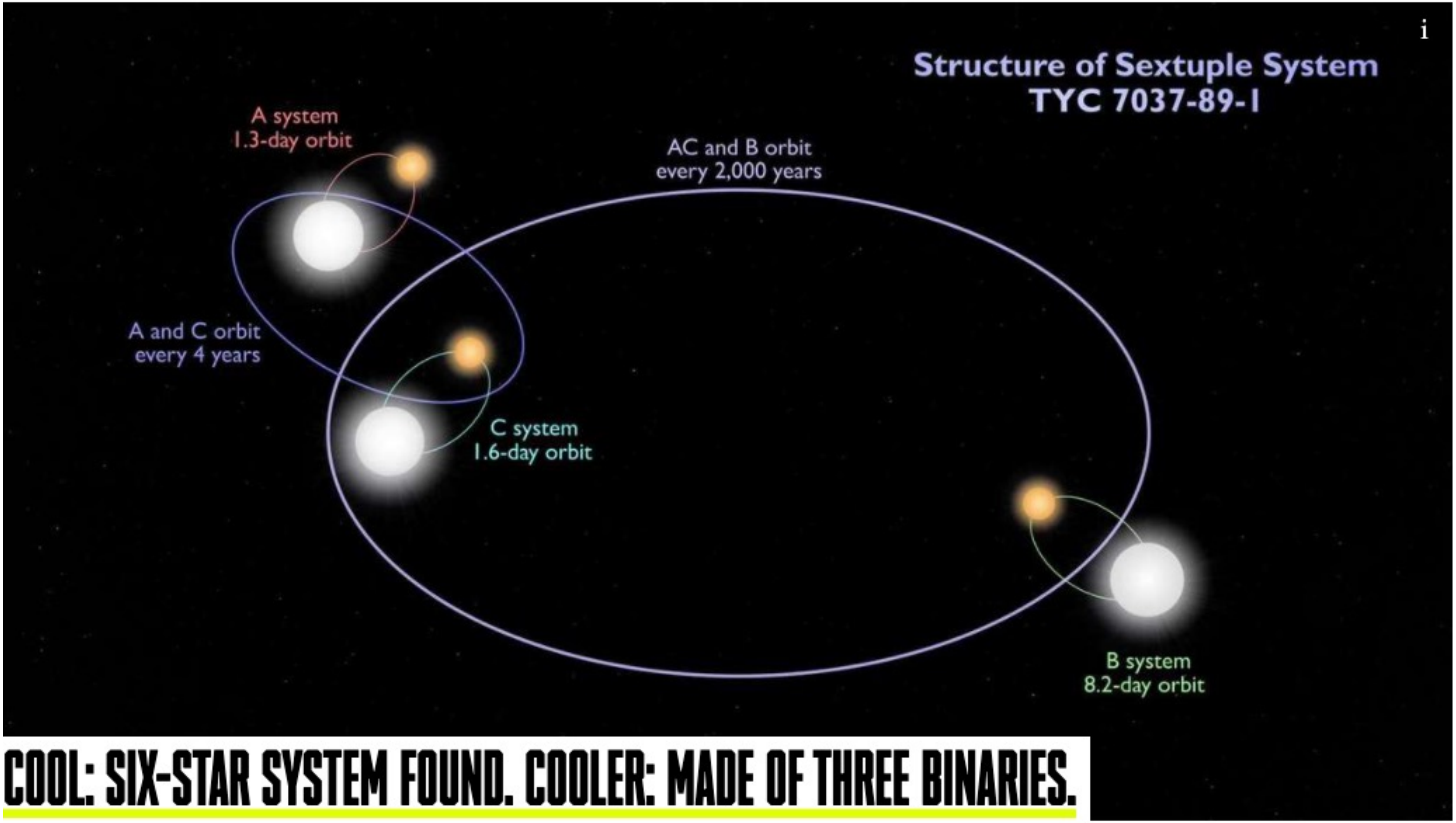

COOL: SIX-STAR SYSTEM FOUND. COOLER: MADE OF THREE BINARIES. COOLEST: *ECLIPSING* BINARIES.

An extreme example: TIC 168789840 – a sextuply eclipsing sextuple star system

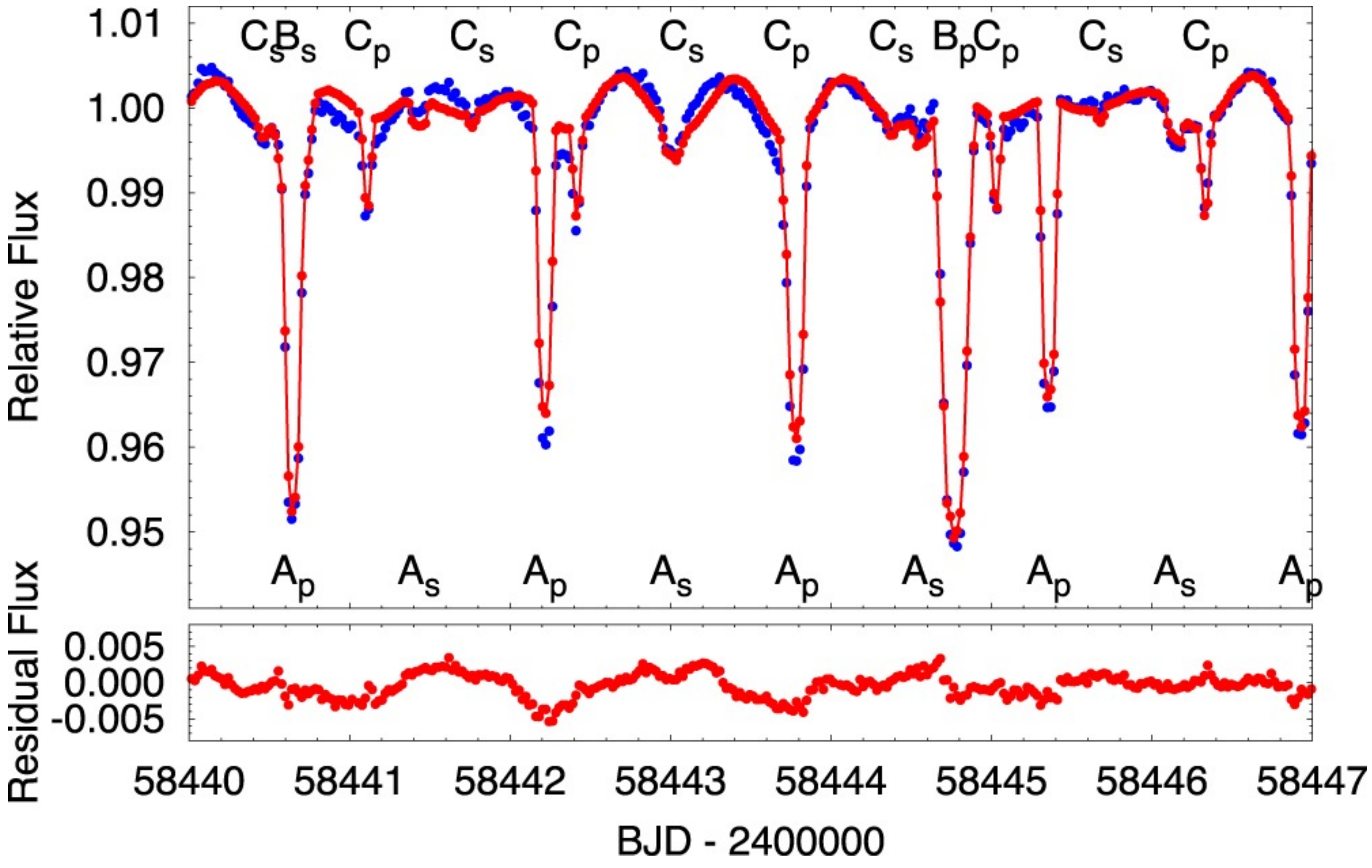

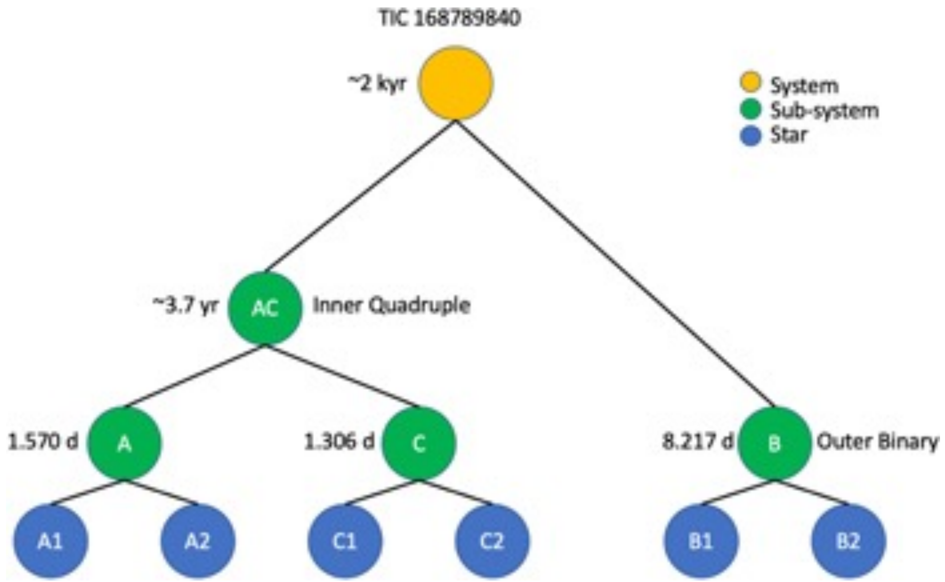

Powell et al. 2021

How can we detect stellar multiplicity?

Detecting stellar multiplicity today

- Direct observation (visual, coronagraphic, interferometric)
- Indirect clues (e.g. shape of nebulae)
- Photometry (eclipses, overluminous, colors)
- Spectroscopy (Doppler shift, multiple components in spectrum)
- Astrometry (displacement on sky)
- Chronometry (light-time effect in pulsating stars)
- Gravitational waves (LISA)

History

- 1767: Rev. John Michell argues many double stars physically close to each other
- 1781: Ch Mayer’s inventory of 80 double stars (speculated about small suns orbiting larger ones in 1779)
- 1782: Discovery of Algol by Goodricke
- 1782: William Herschel 269 visual binaries
- 1803: Herschel finds that some double stars change relative position
- 1803: Herschel defines “binary star”= “a real double star – the union of two stars that are found together in one system, by the laws of attraction” (posits universality of gravitational attraction!!)

History

- 1837: Wilhelm Struve detected about 3,000 double stars
- Sons John Herschel & Otto Struve continued & expanded fathers’ legacies
- 1842: Christian Doppler considered color change due to orbital motion
- Bessel, Auwers, Clark measured variable proper motion of Sirius due to WD companion at 7.5”
- 1905: Burnham publishes General Catalog of (13,665) Double Stars within 121deg of North Pole

Friedrich Georg Wilhelm von Struve

History

- 1889: Charles Pickering (Harvard) finds first SB2 (Mizar)
- 1889: Herrmann Carl Vogel (Potsdam) finds first SB1 (Spica)
- The hunt for spectroscopic binaries begins…
- 1905: Campbell & Curtis: First catalogue of (140) spectroscopic binaries based on Mills spectrograph @ Lick Observatory
- Duquennoy & Mayor (1991): 60% of solar-type stars are binaries!
- Nowadays: are all massive stars binaries?
- Moe & DiStefano (2017): detailed review of multiplicity fractions across mass ranges & evolutionary stages

δ Ori: discovery of the ISM by Hartmann

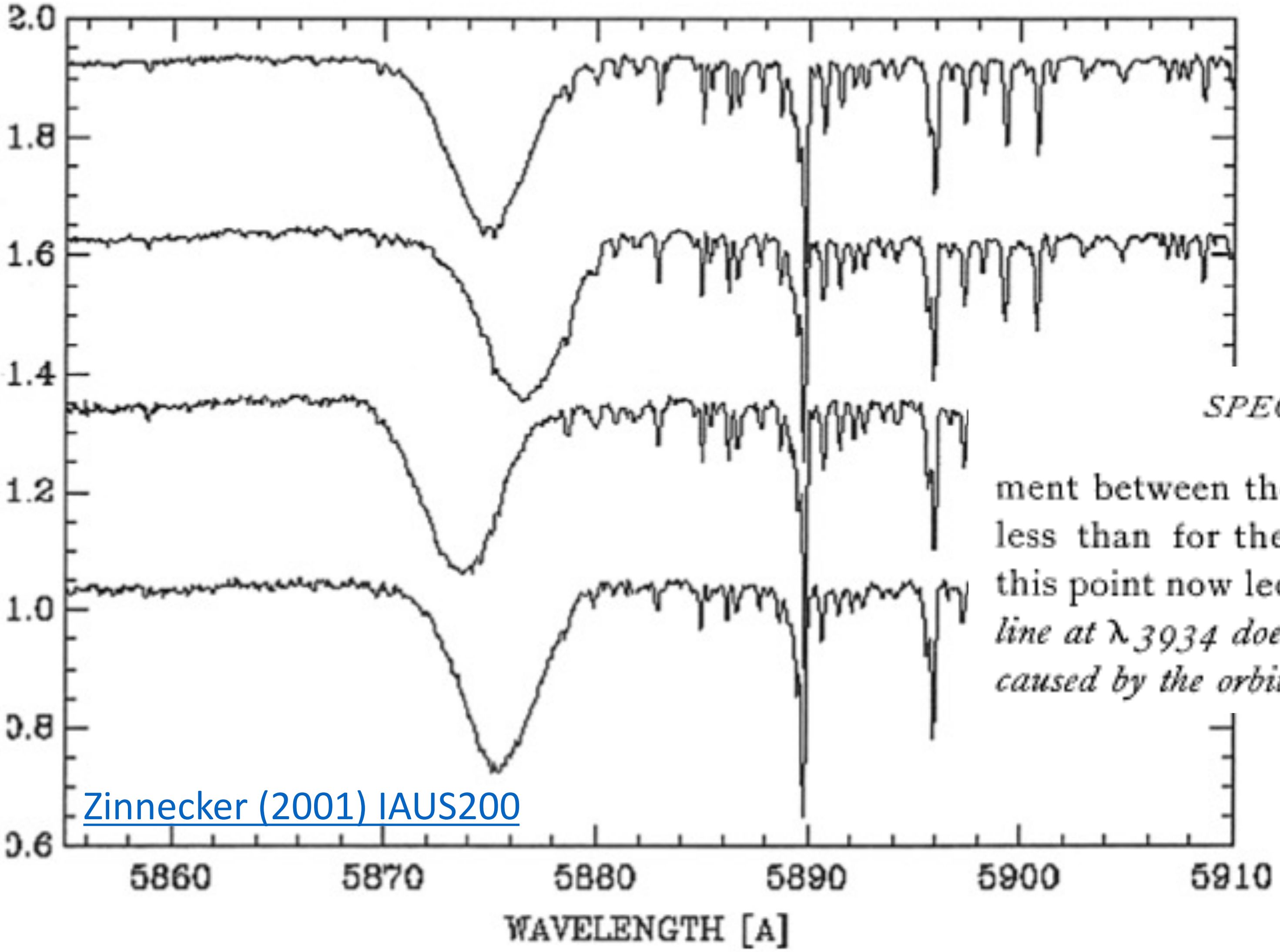

[Zinnecker (2001) IAUS200]

used "oscillation" in favor of "variability of velocity in the line of sight" to avoid explaining phenomenon

SPECTRUM AND ORBIT OF δ ORIONIS 273

ment between the results from the different plates was decidedly less than for the other, much less sharp lines. Closer study on this point now led me to the quite surprising result *that the calcium line at λ 3934 does not share in the periodic displacements of the lines caused by the orbital motion of the star.*

[Hartmann 1904]

Spectroscopic binaries: double-lined

Gaia DR4 will have billions of epoch spectra from RVS instrument

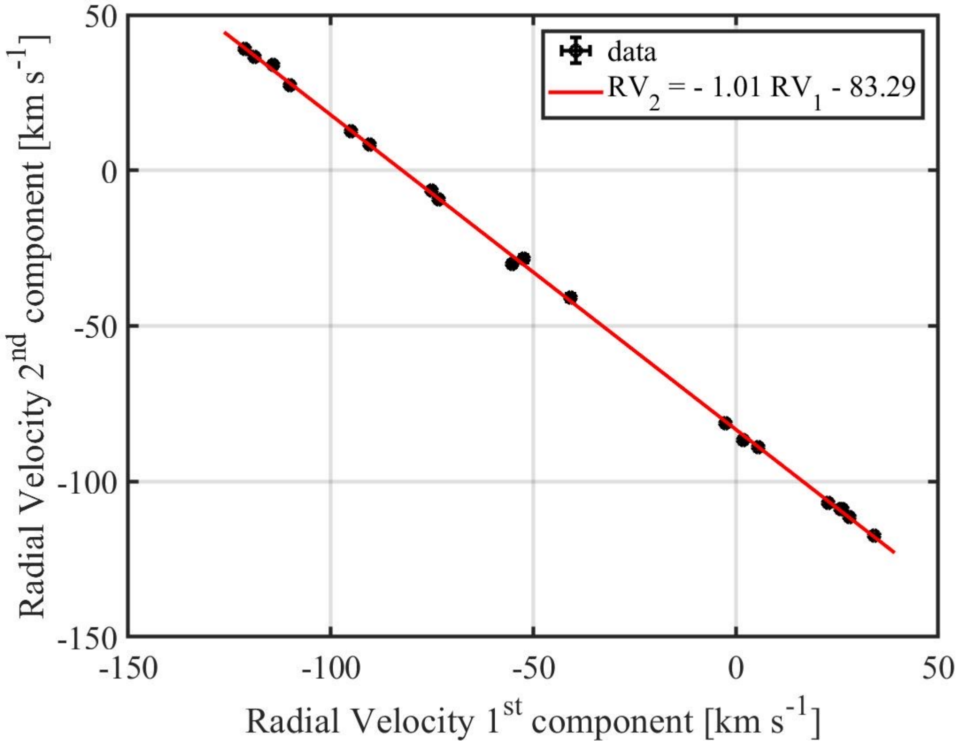

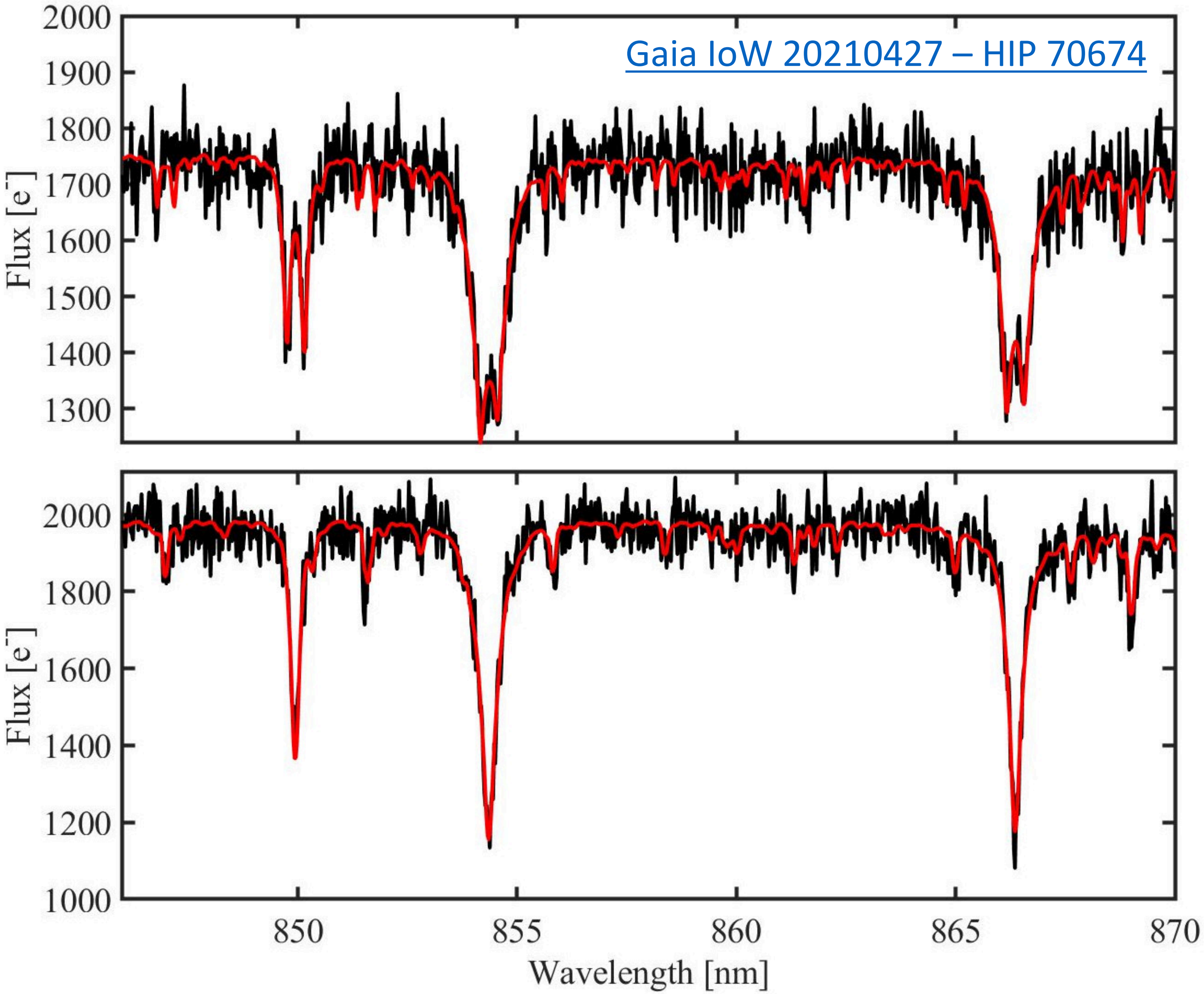

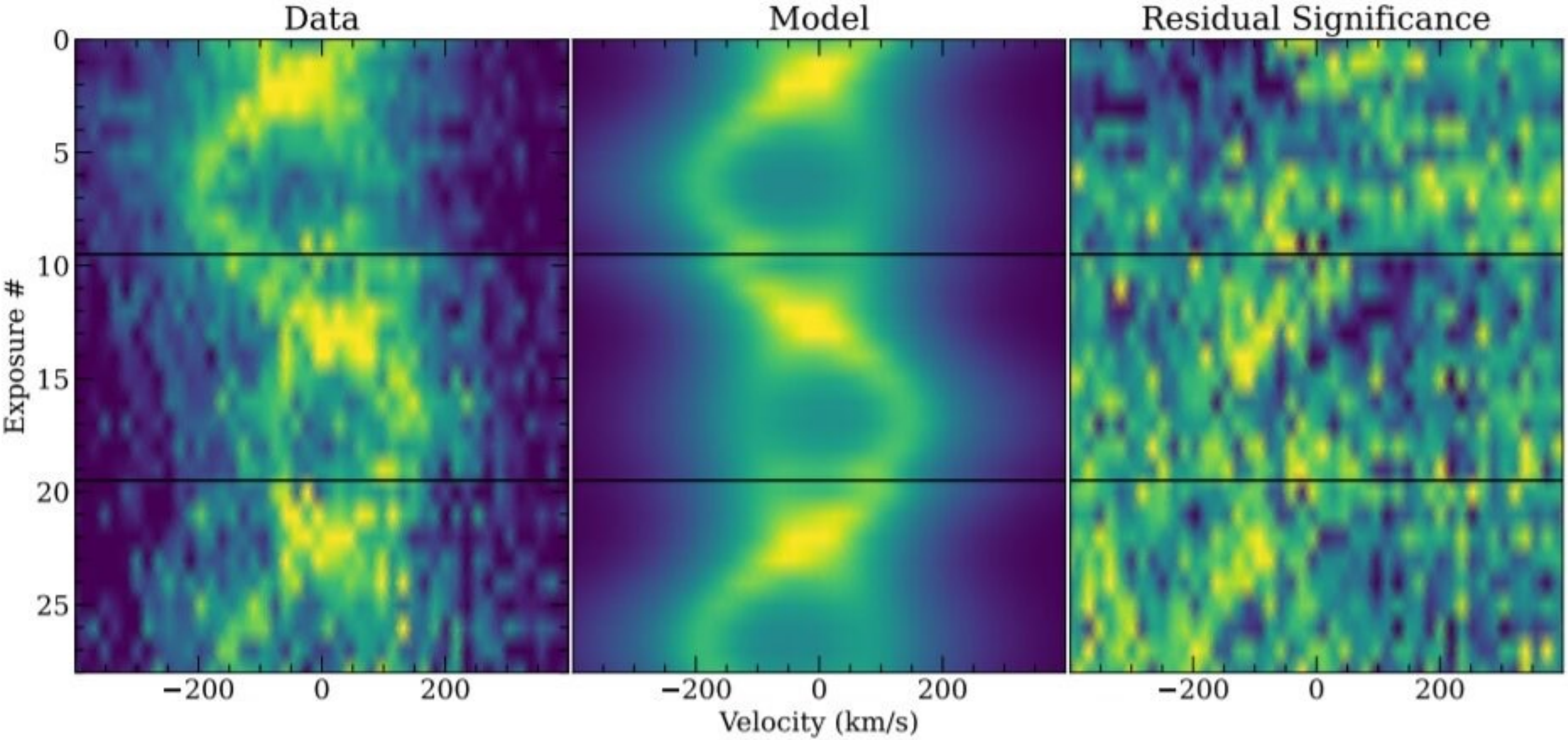
Data
Model
Residual Significance
Exposure #
0
5
10
15
20
25
−200
0
200
−200
0
200
−200
0
200
Velocity (km/s)

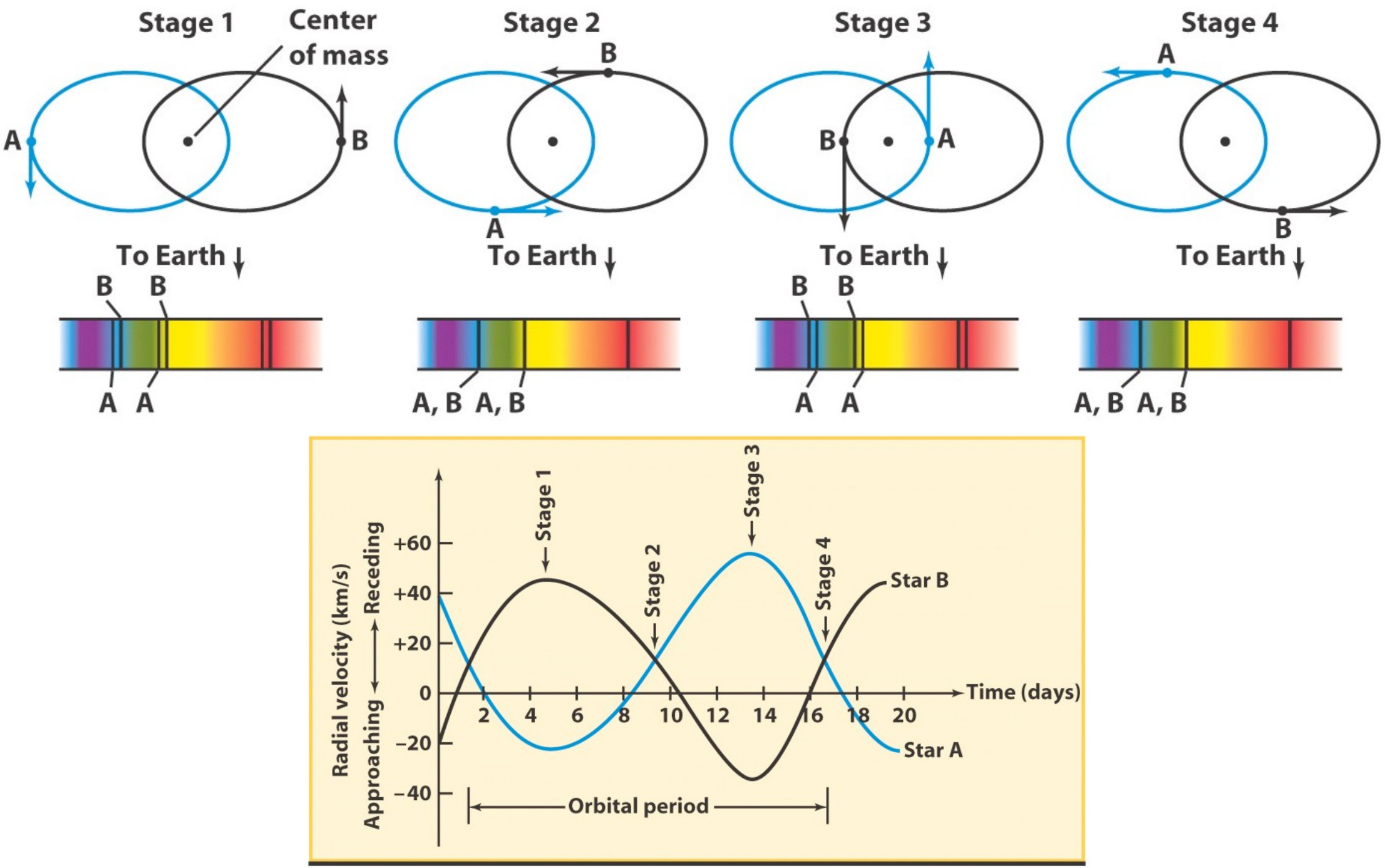

Stage 1
Center of mass
Stage 2
Stage 3
Stage 4
A
B
To Earth
A, B
Radial velocity (km/s)
Approaching
Receding
+60
+40
+20
0
−20
−40
2 4 6 8 10 12 14 16 18 20
Time (days)
Star A
Star B
Orbital period

[Gaia IoW 20210427 – HIP 70674]

Spectroscopic binaries: double-lined

$$K_l = \frac{2\pi a_l \sin i}{P \cdot \sqrt{1-e^2}}$$

$$f(M) = \frac{(1-e^2)^{3/2} P K^3}{2\pi G}$$

$$M_1 + M_2 = \frac{P}{2\pi G}\frac{(v_1+v_2)^3}{\sin^3 i}$$

$$\frac{M_1}{M_2} = \frac{K_2}{K_1} = \frac{a_2}{a_1}$$

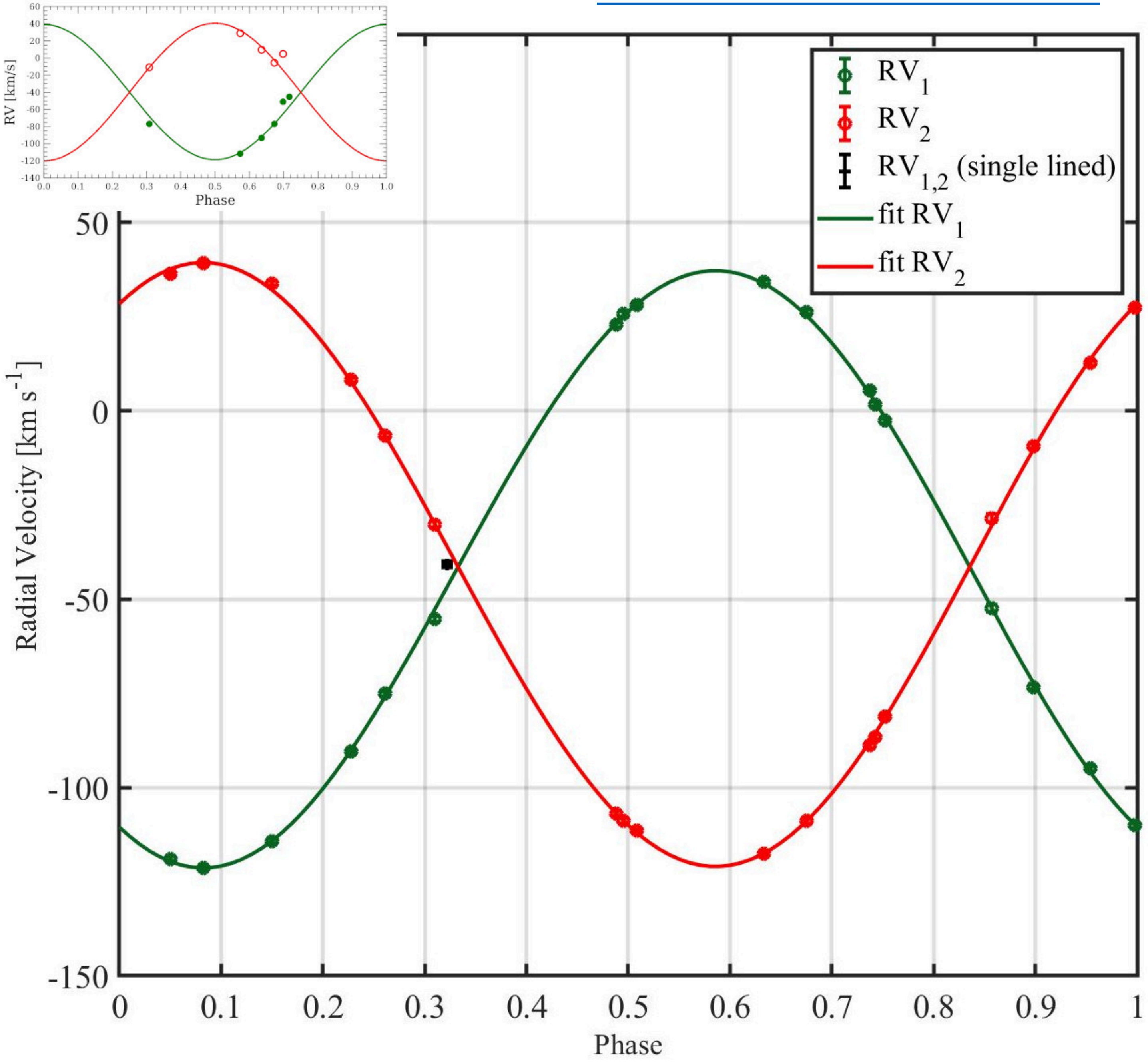

Astrometric / visual binaries

Kervella et al. (2019)

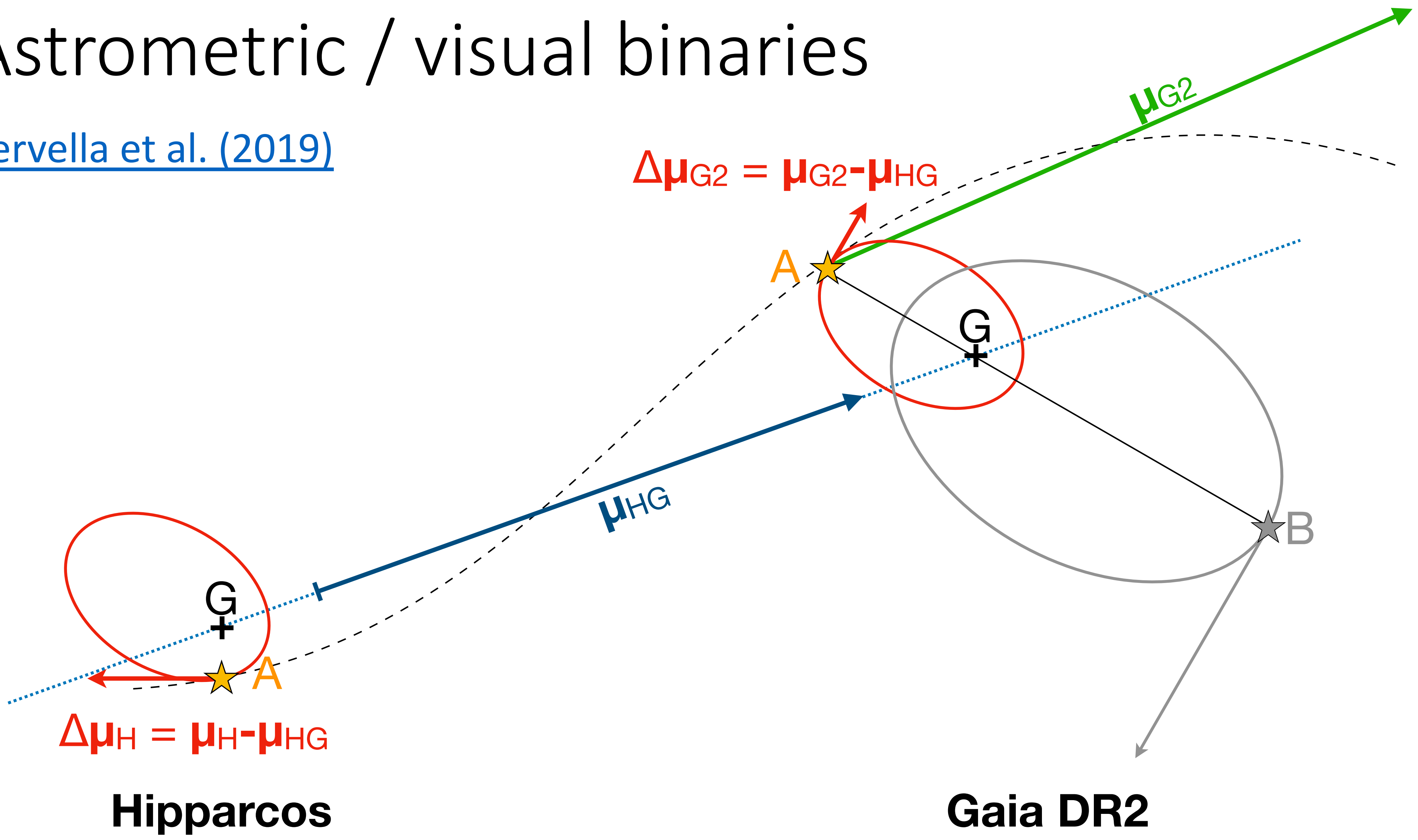

Astrometric binaries

[Kervella et al. (2019)](#)

$$4\pi^2 a_{rel}^3 = GM_{tot}P^2$$

$$a_{rel} = a_1 + a_2$$

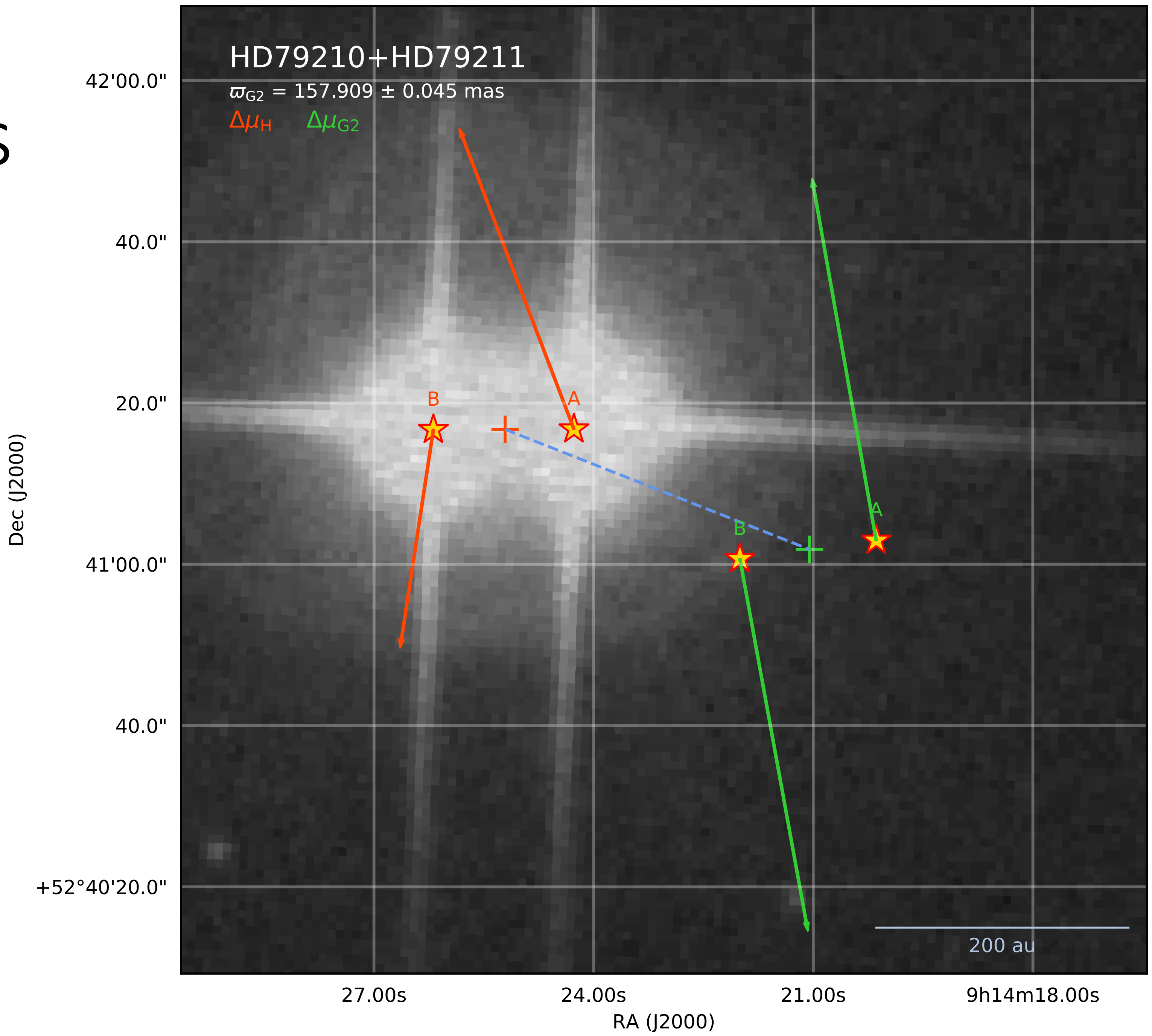

Gaia DR3 now has non-single star solutions!

$P = 850.84 \pm 112.53$ d
$e = 0.37 \pm 0.15$
$T_{\mathrm{P}} = 145.68 \pm 68.64$ d
$\alpha = 0.40^{+0.03}_{-0.03}$ mas
$\omega = 63.22^{+13.91}_{-14.84}$ deg
$\Omega = 12.46^{+5.79}_{-5.38}$ deg
$i = 107.40^{+5.51}_{-5.58}$ deg

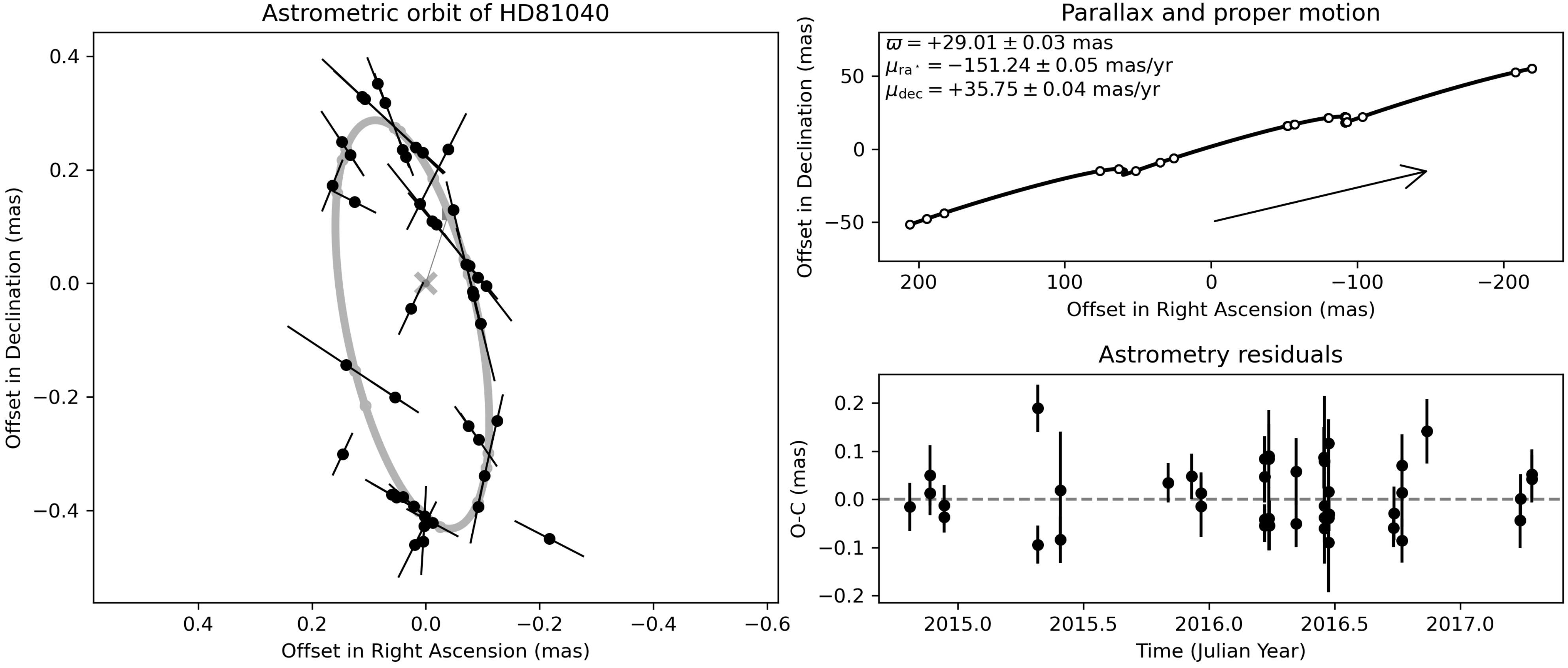

335 solved astrometric orbits in Gaia DR3

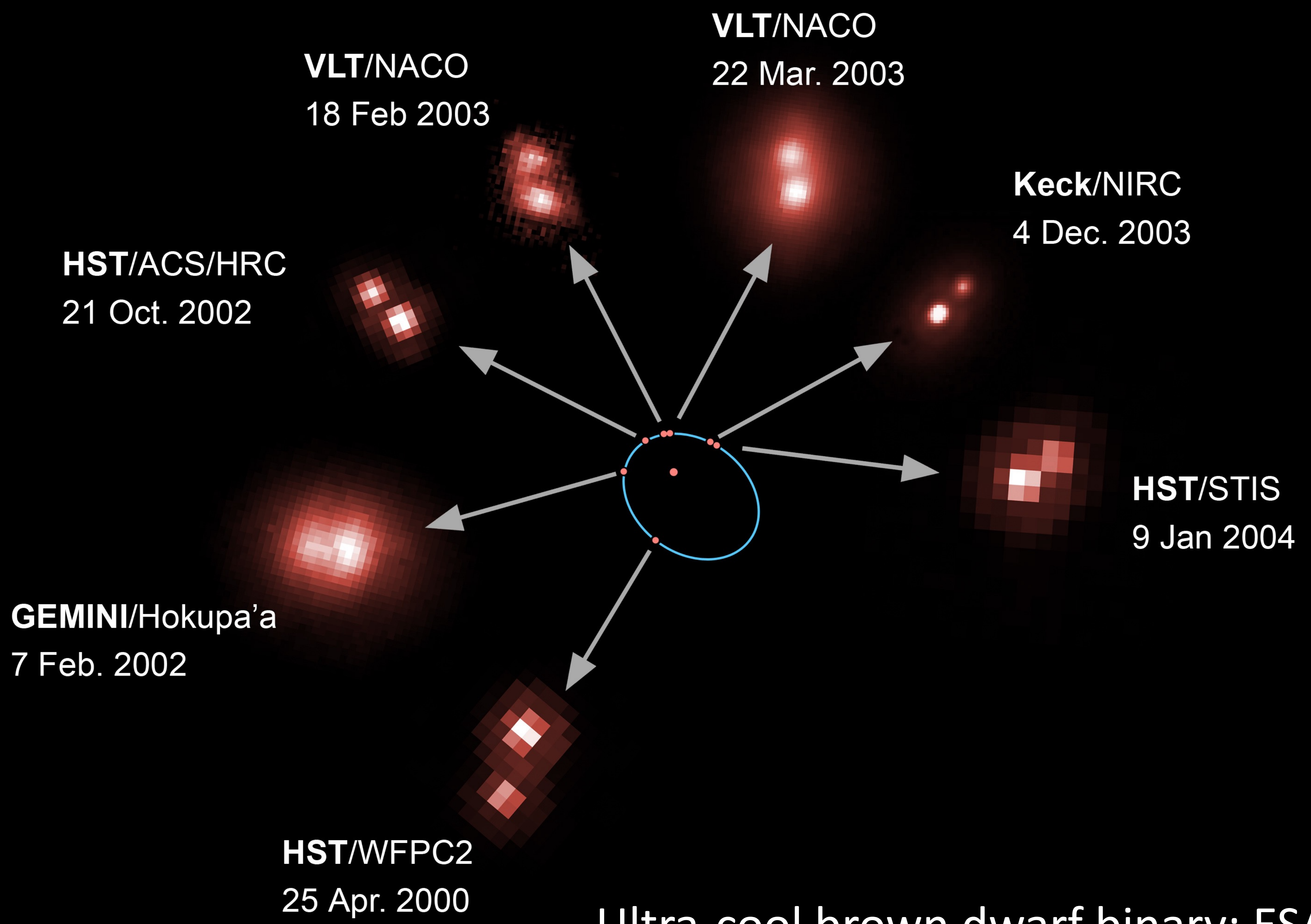

Ultra-cool brown dwarf binary: ESA

Eclipsing binaries

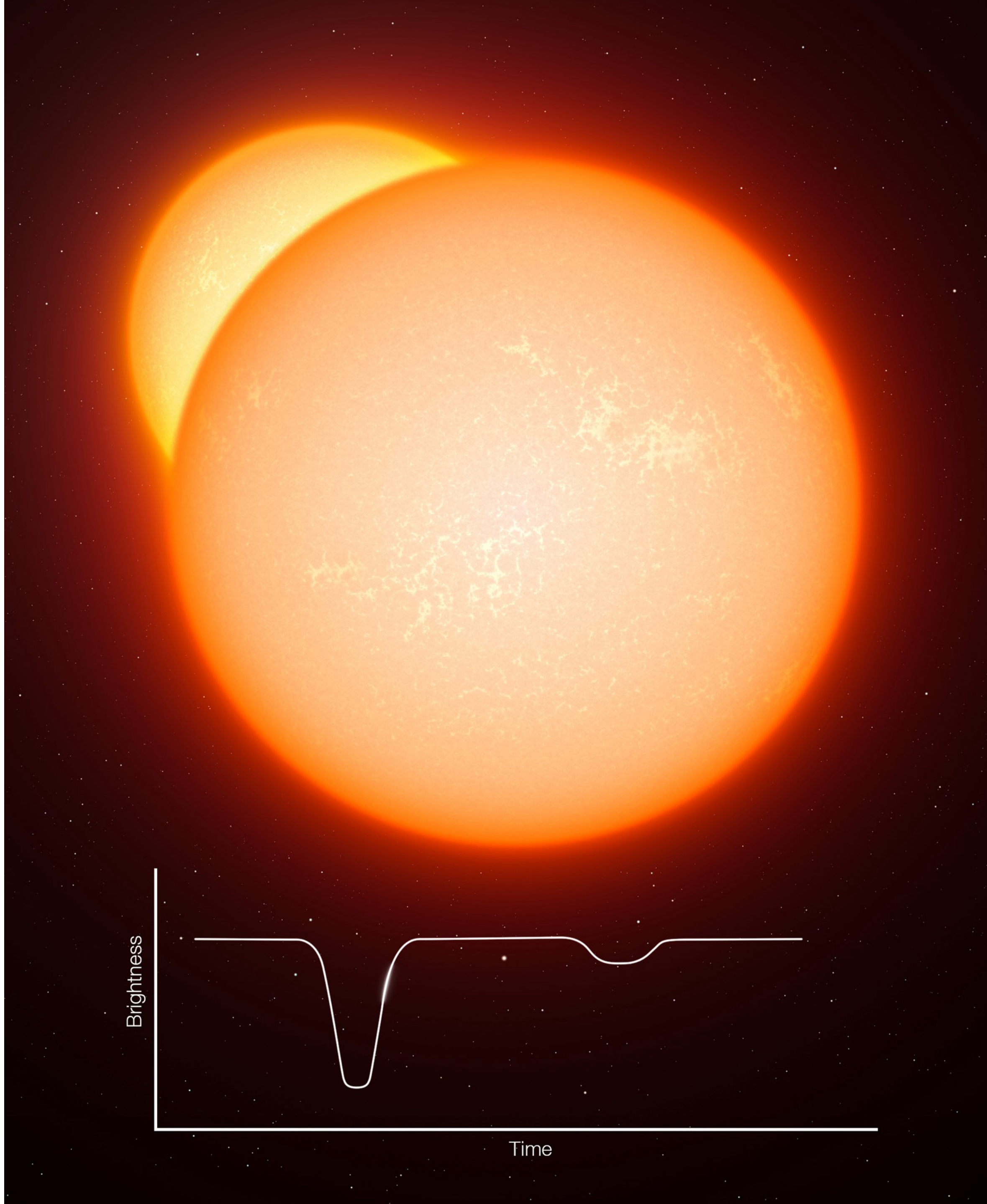

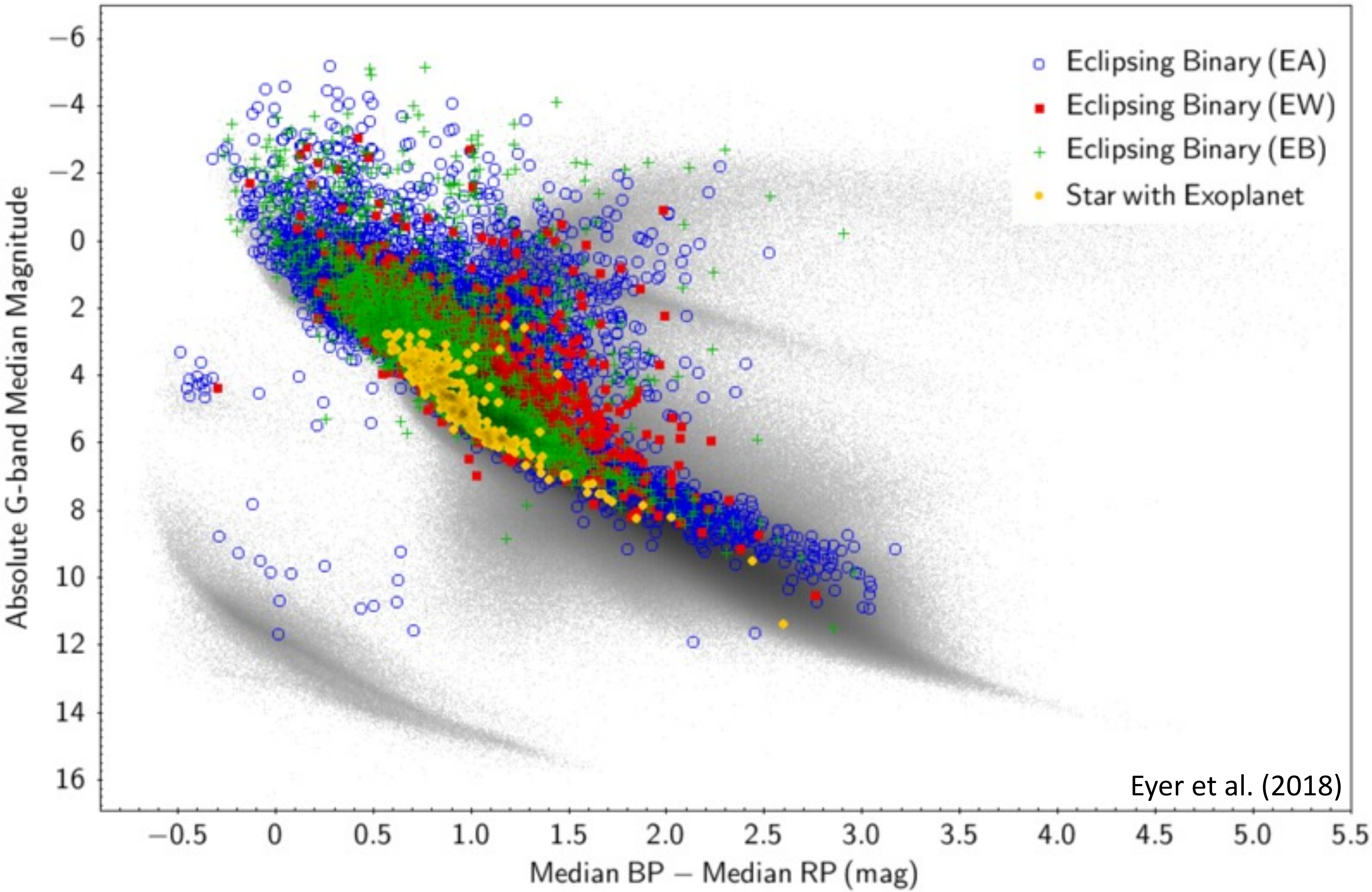

Eyer et al. (2018)

Gaia’s binaries

- Gaia DR3 delivered
  - Eclipsing
  - Spectroscopic
  - Astrometric binaries
- Volumes probed differ
- Selection effects differ
- Limited by
  - Magnitudes
  - Timescales
  - distances

Gaia Collaboration, Arenou, F., et al. 2022

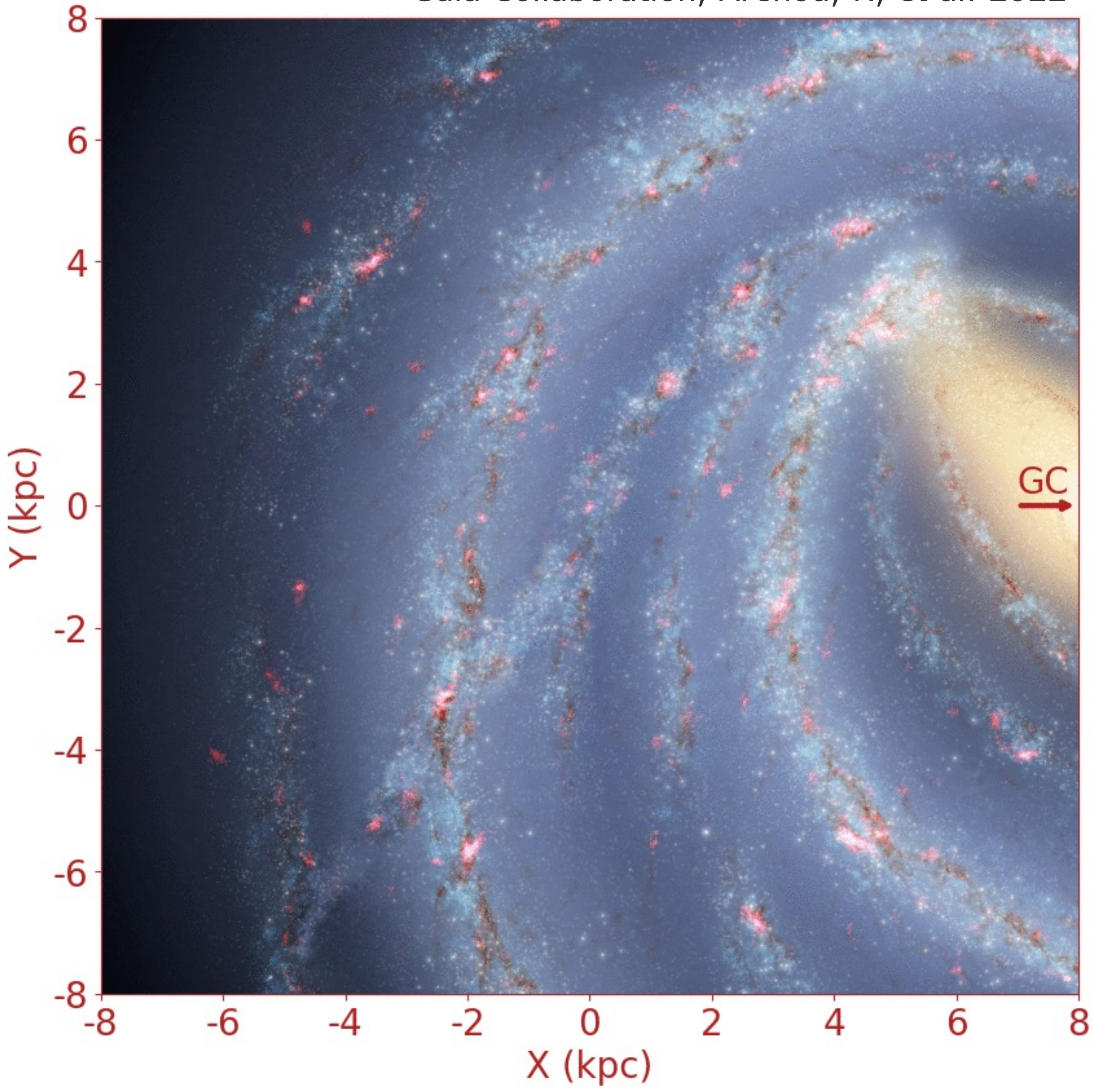

Reasons to study eclipsing binaries (incomplete)

Binary fractions

Orbit configurations

Stellar sizes

Absolute mass

System characterization

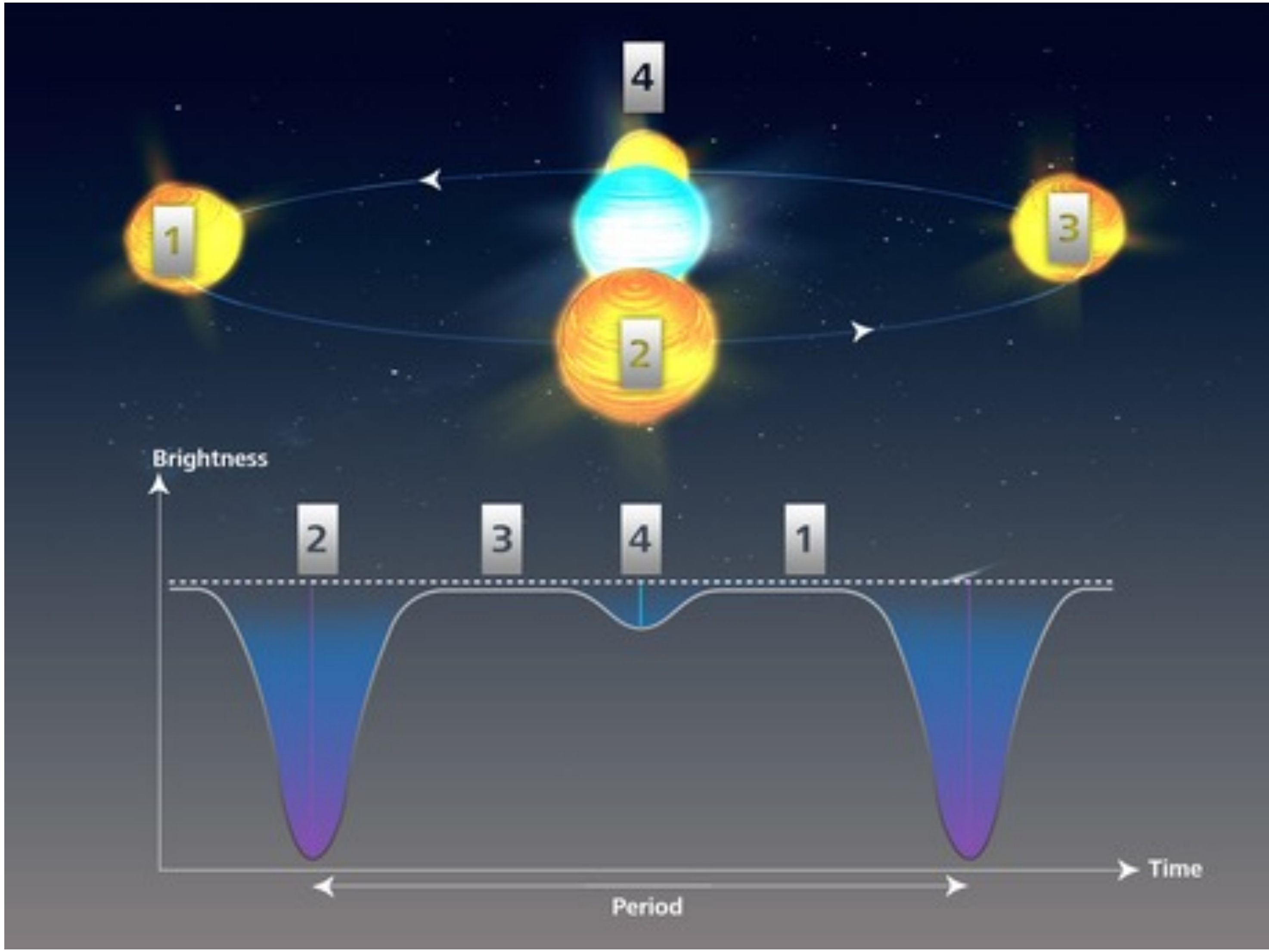

Radii from Detached Eclipsing Binaries

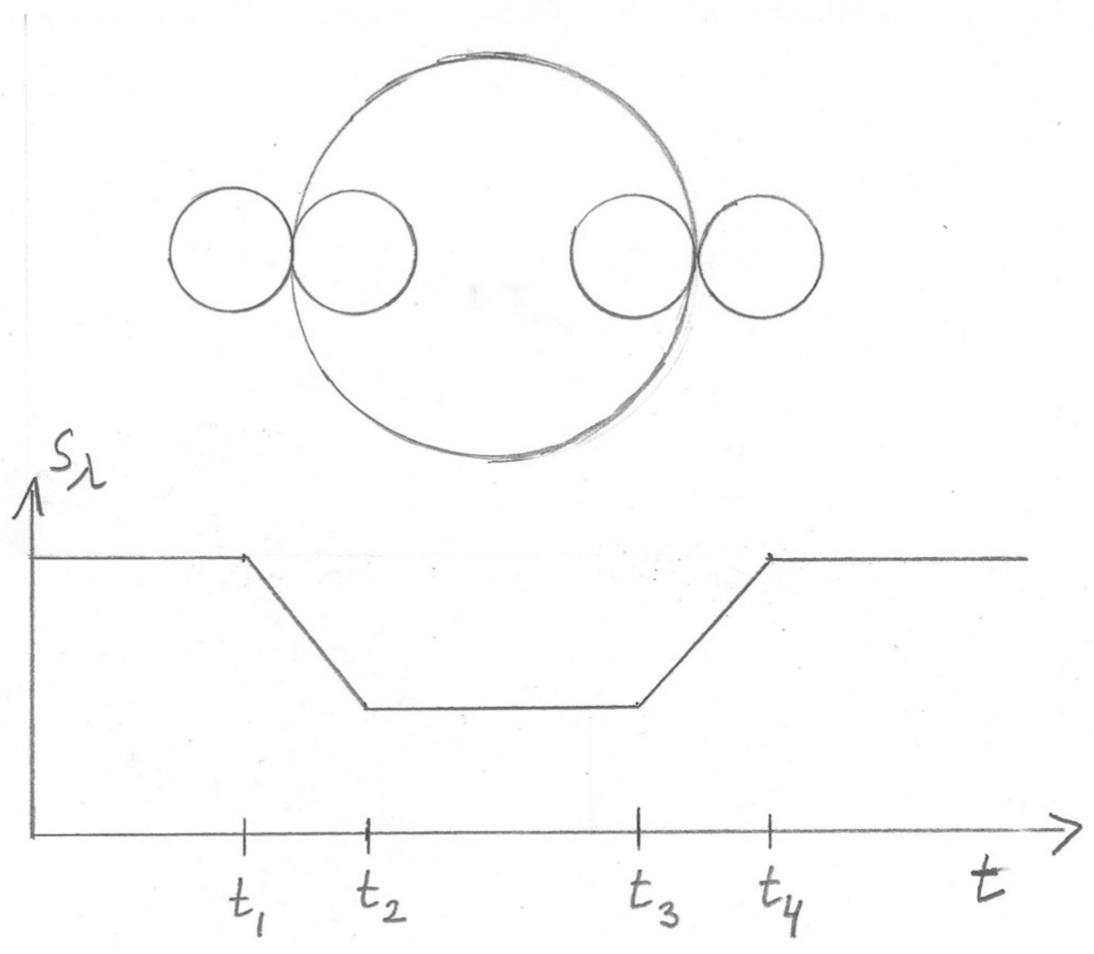

Total eclipse duration:

$$\frac{t_4 - t_1}{P} = \frac{2R_1 + 2R_2}{l}$$

Minimum of eclipse duration:

$$\frac{t_3 - t_2}{P} = \frac{2R_1 - 2R_2}{l}$$

Path along orbit during eclipse:

$$l = 2\pi a_{rel} = P(v_1 + v_2)$$

Mass from SB2:

$$M_1 + M_2 = \frac{P}{2\pi G} \frac{(v_1 + v_2)^3}{\sin^3 i}$$

Diversity of eclipsing systems

The Roche equipotential surfaces

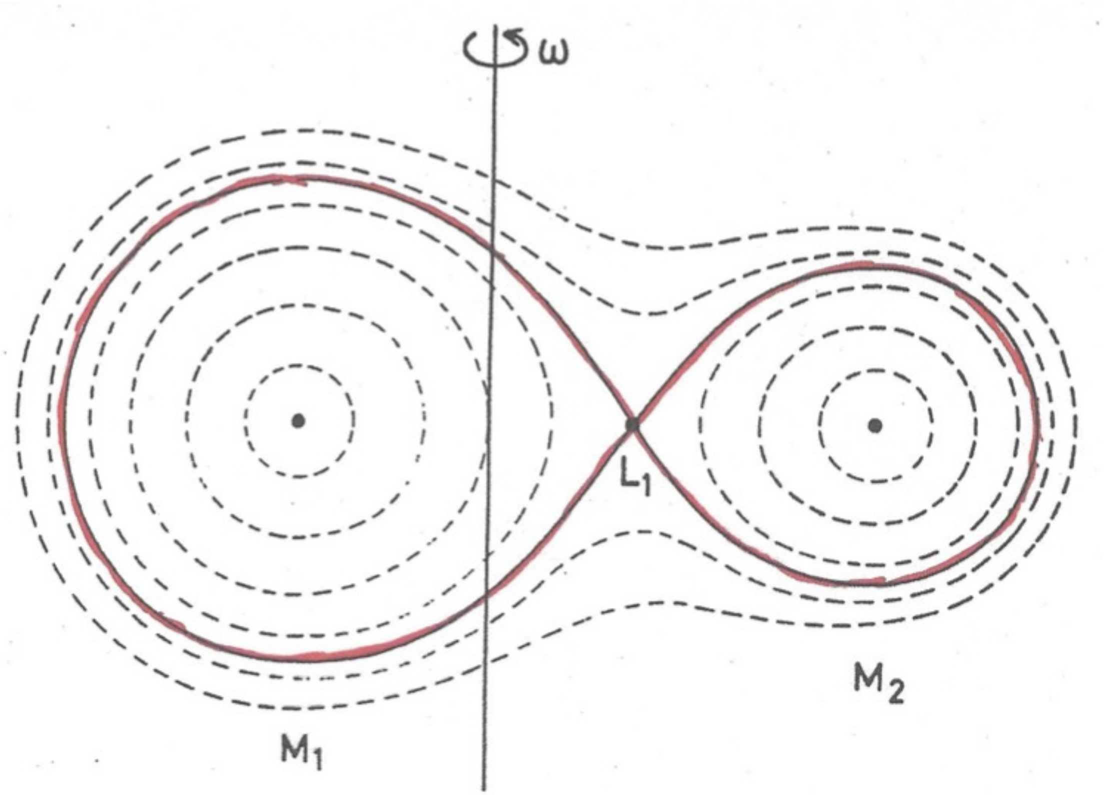

- Determine sphericity of stars
- Larger diameters / closer approaches -> deviations from spherical
- No gravitational attraction at L_1
- Inside Roche surface matter is bound to either star 1 or 2

EA eclipsing binaries

- Prototype: Algol
- Spherical or ellipsoidal components
- Well-separated
- Light curve nearly constant between minima
- Secondary minima can be absent

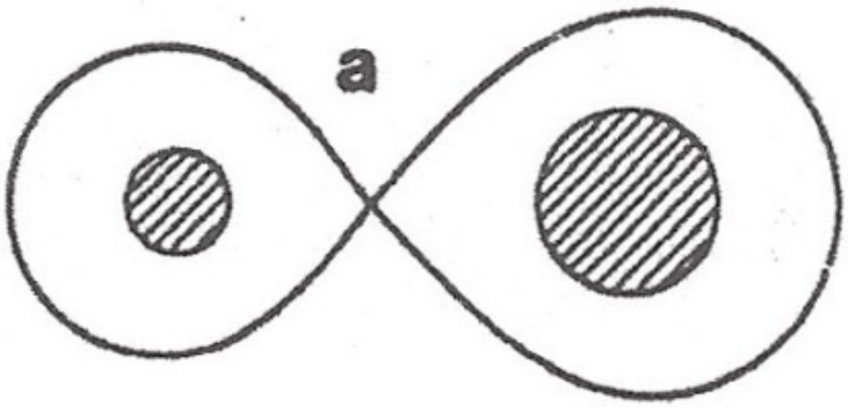

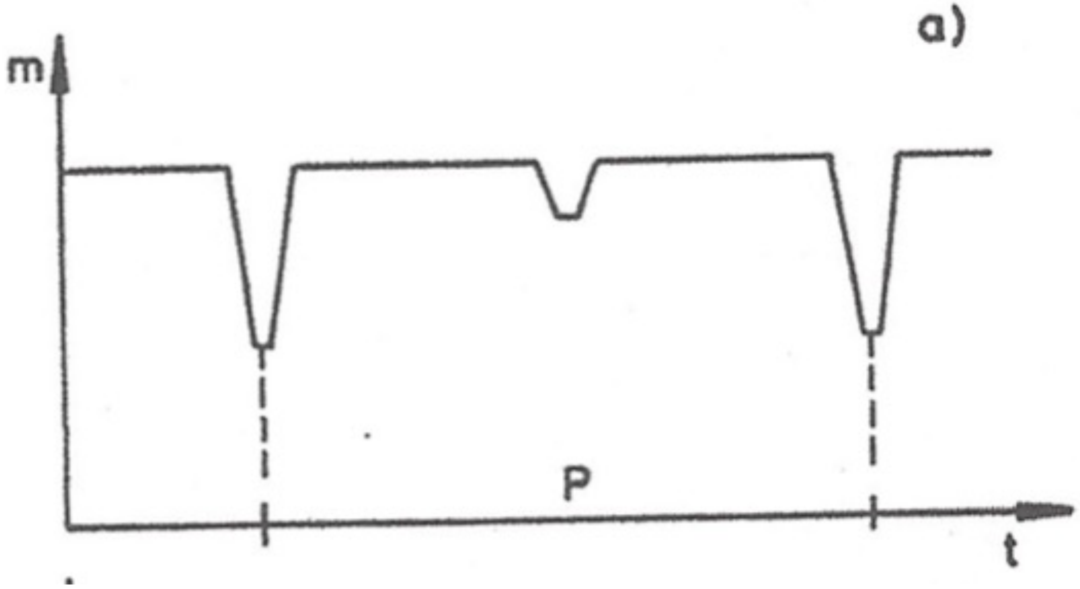

EB eclipsing binaries

- Prototype: β Lyrae
- Light curve continuously changing
- Onset or end of eclipses not clearly defined
- Secondary eclipses always present (can be shallow)

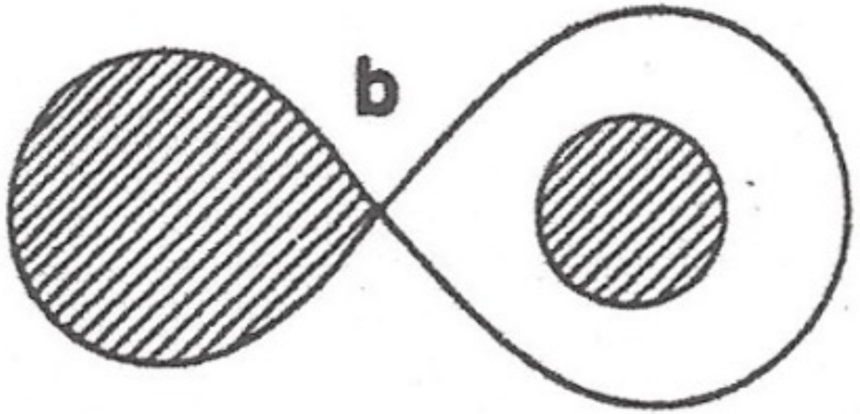

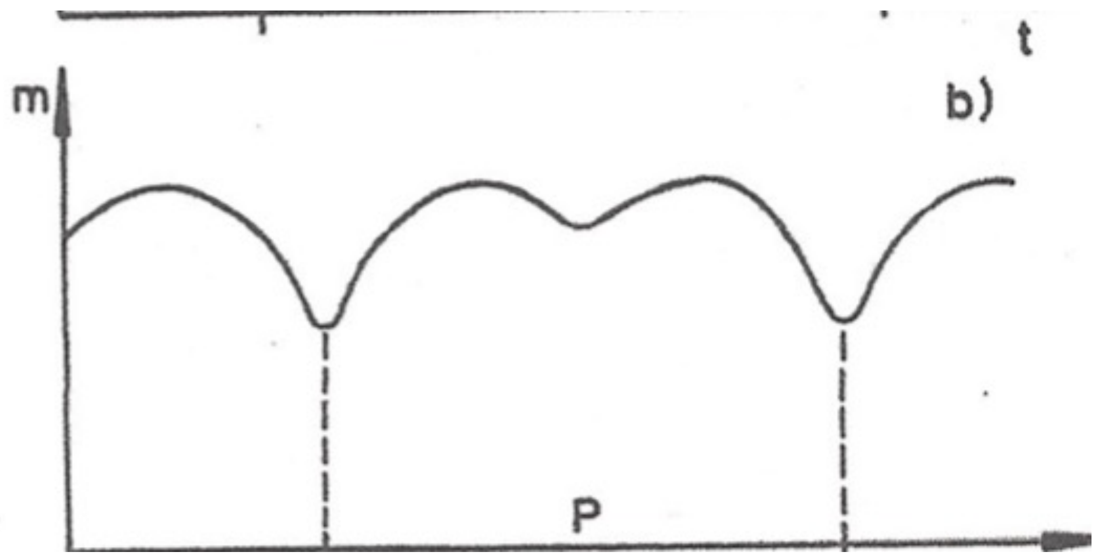

EW eclipsing binaries

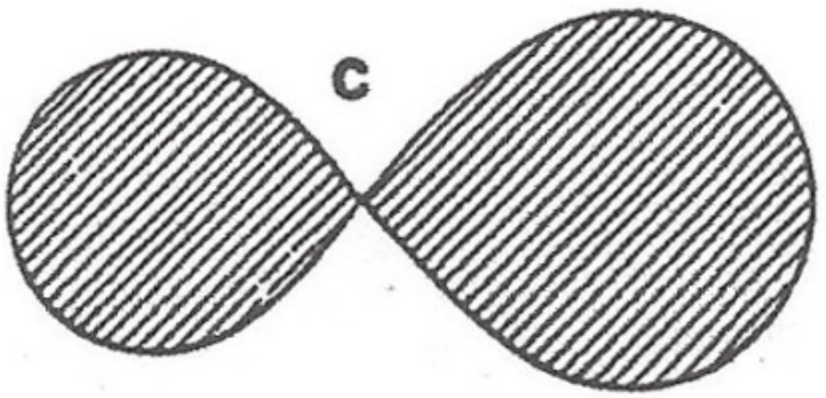

- Prototype: W Ursae Majoris
- Components nearly or actually in contact
- Minima equally strong
- Onset and ends of minima not clearly defined

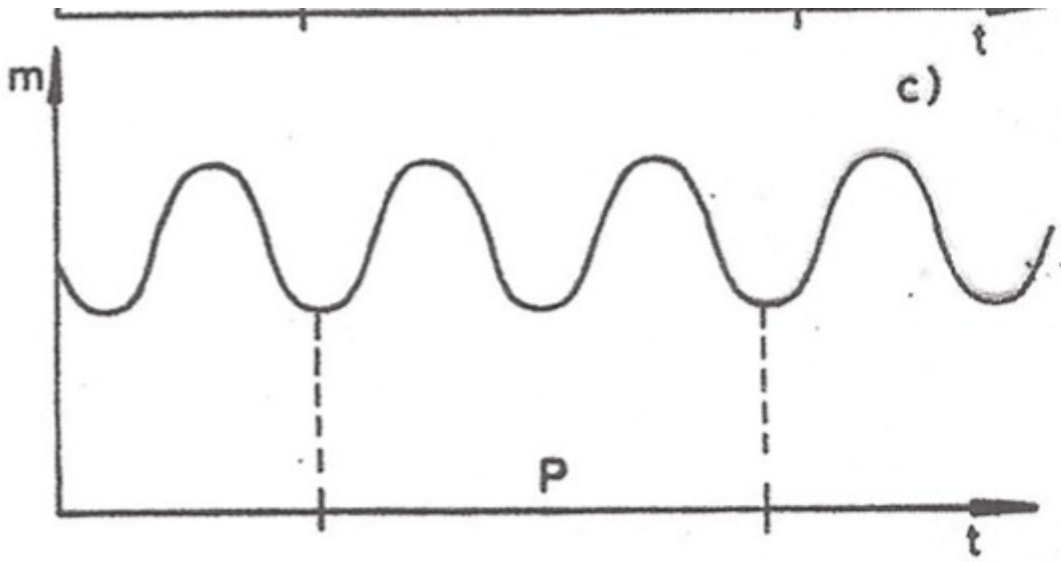

Apsidal motion

- Precession of line of apsides
- ω: argument of periapsis
- $\omega_{tot} = \omega_{GR} + \omega_{quad} + \omega_{tide} + \omega_{perturb}$
- $\dot{\omega}$: apsidal precession
- $\dot{\omega}_{GR} = \frac{24\pi^3 a^2}{T^2 c^2 (1-e^2)} = \frac{43''}{100yr}$ [Mercury]

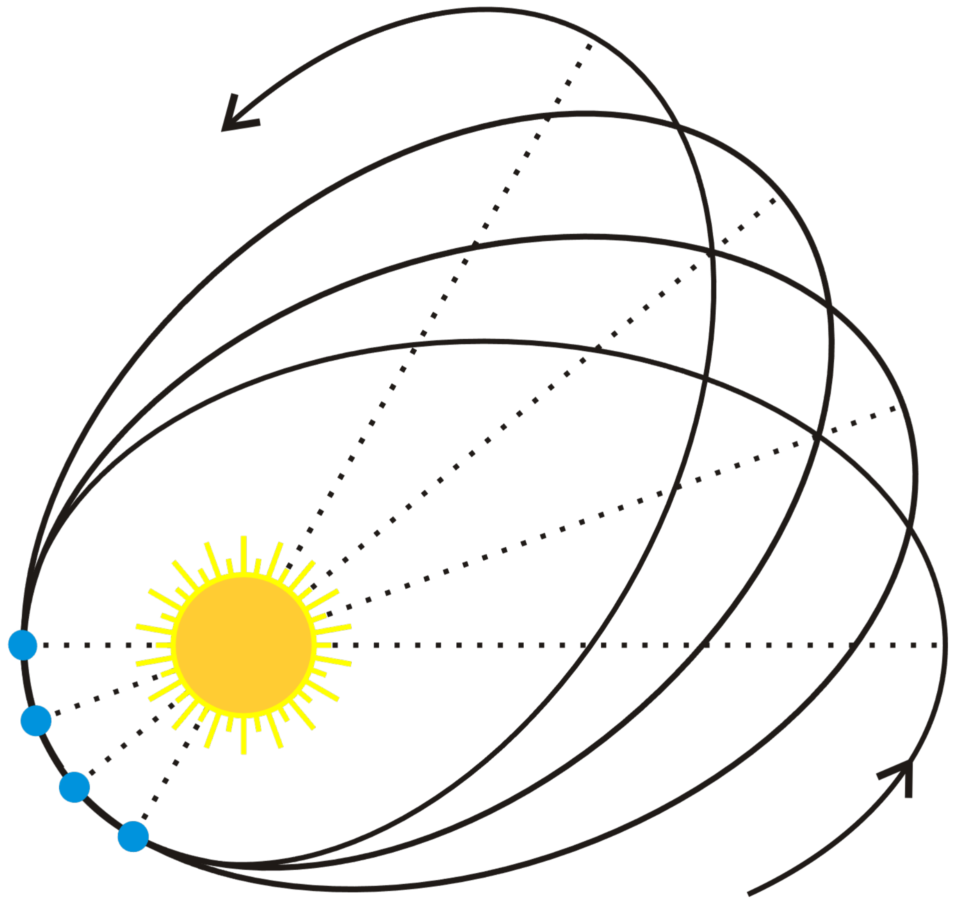

Zasche et al. (2020)

Apsidal motion

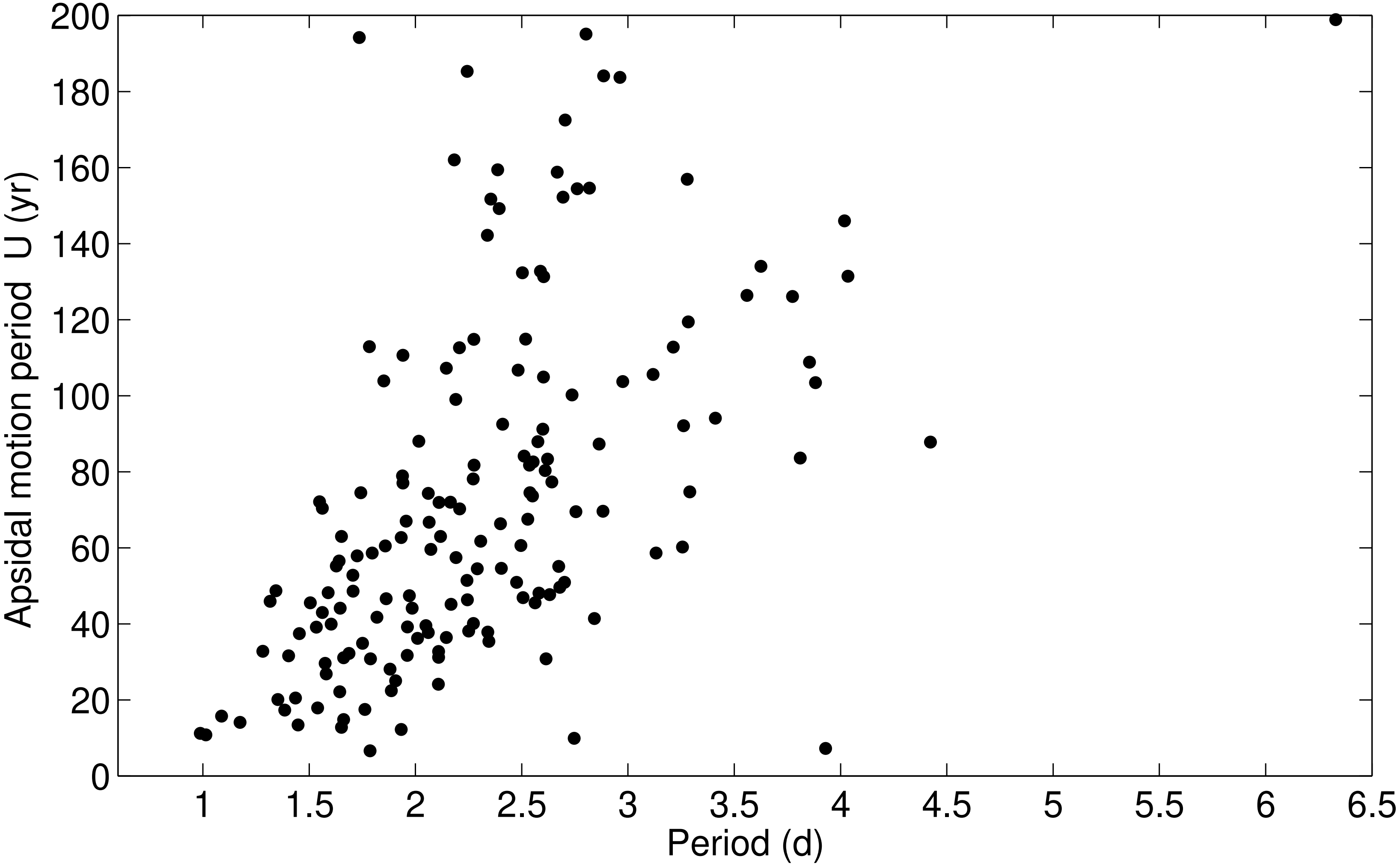

Apsidal motion from Eclipse Timing Variations

Zasche et al. (2020)

$$(O - C) = JD_i - HJD_0 - P \cdot E - (O - C)_{LTE} - (O - C)_{AM}$$

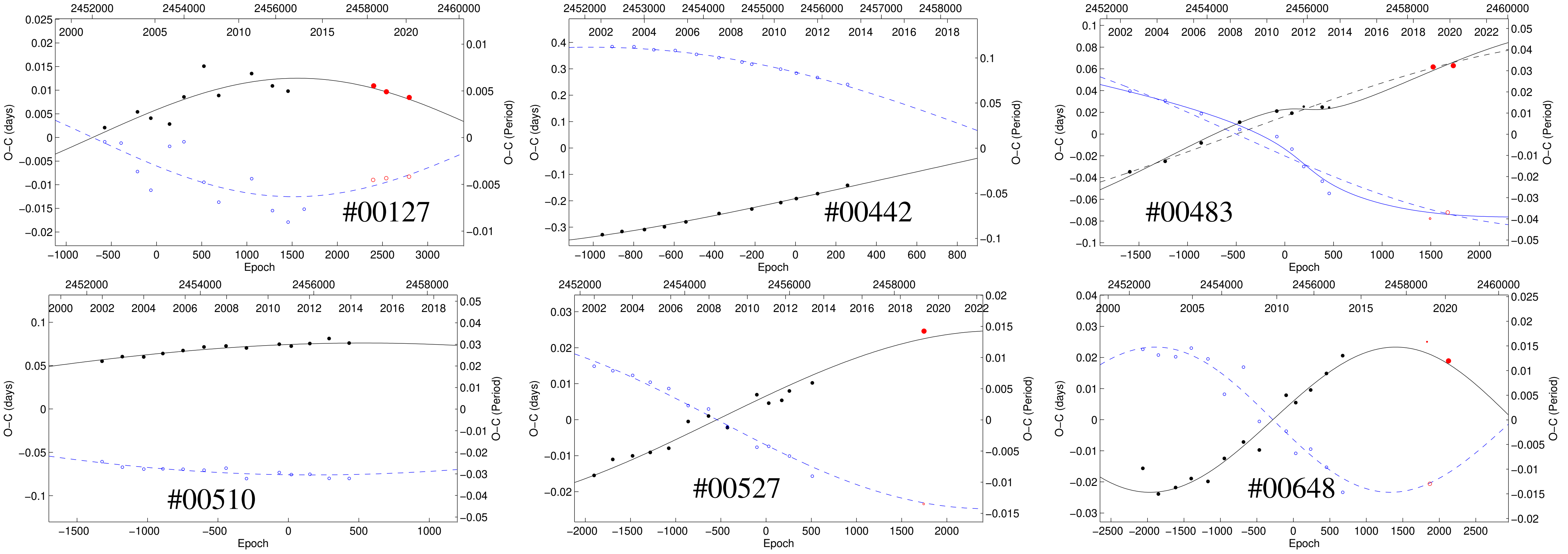

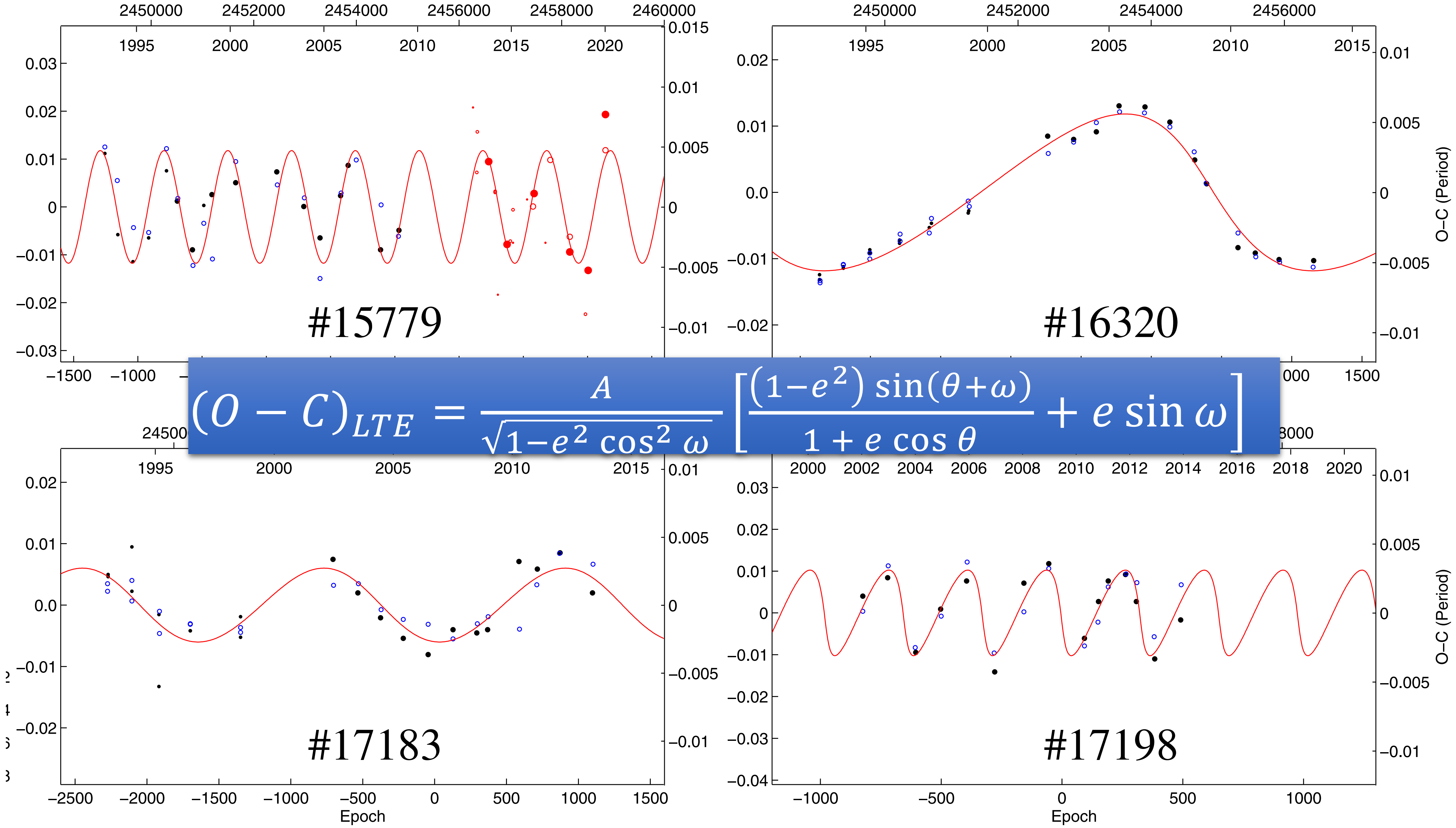

$$(O-C)_{LTE} = \frac{A}{\sqrt{1-e^2\cos^2\omega}}\left[\frac{(1-e^2)\sin(\theta+\omega)}{1+e\cos\theta} + e\sin\omega\right]$$

Part II: Rotational variables

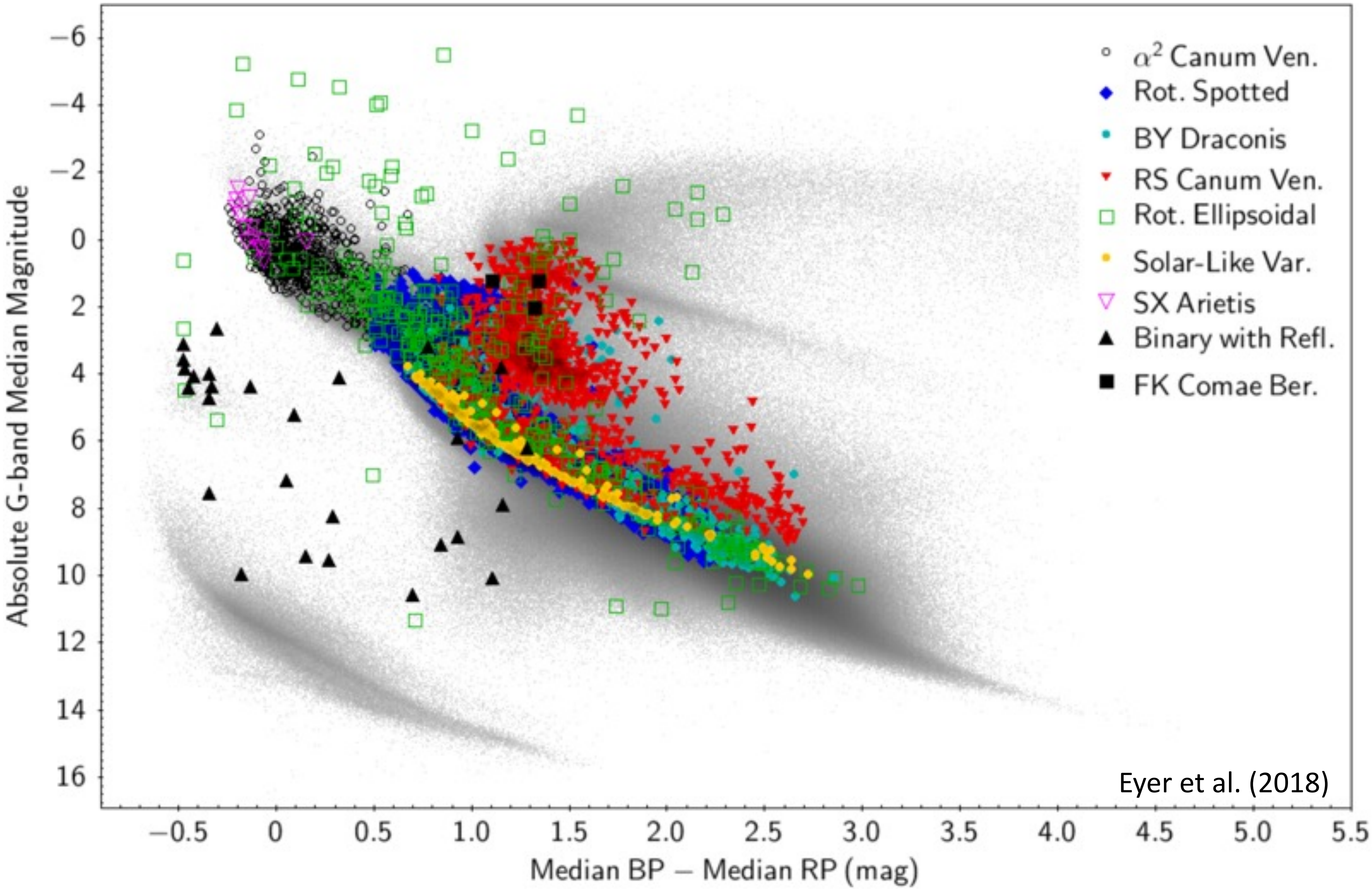
α² Canum Ven.
Rot. Spotted
BY Draconis
RS Canum Ven.
Rot. Ellipsoidal
Solar-Like Var.
SX Arietis
Binary with Refl.
FK Comae Ber.
Absolute G-band Median Magnitude
Median BP − Median RP (mag)
−6
−4
−2
0
2
4
6
8
10
12
14
16
−0.5
0
0.5
1.0
1.5
2.0
2.5
3.0
3.5
4.0
4.5
5.0
5.5
Eyer et al. (2018)

Variability by spot rotation

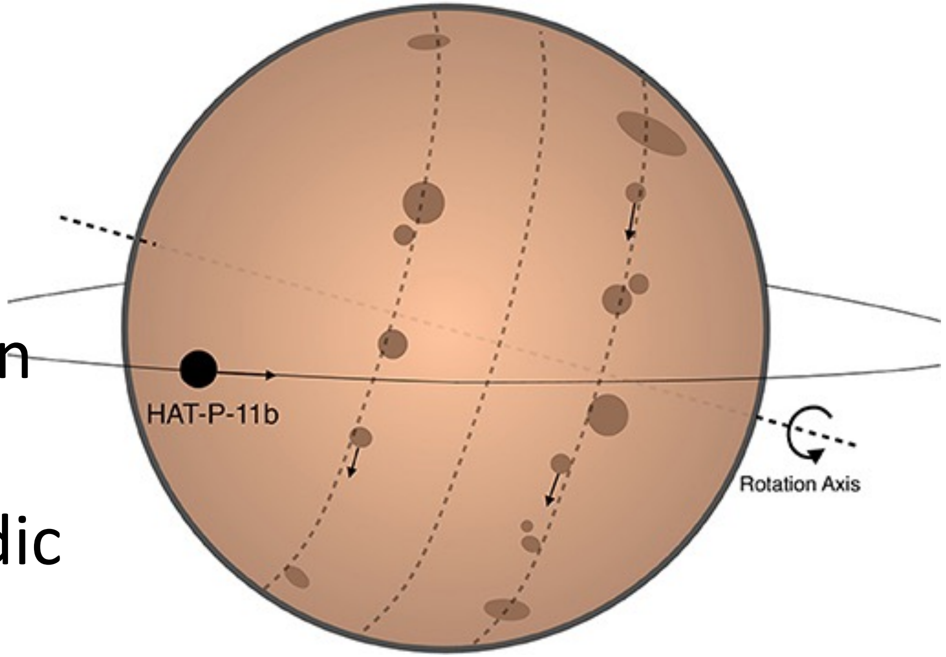

- **Spotted MS stars**: rotational light modulation
- **BY Draconis**: K & M MS stars featuring spots & chromospheric activity; quasi-periodic
- **RS Canum Venaticorum**: spots + eclipses and flares
- **FK Comae Berenices**: rapidly rotating with non-uniform surface
  - G-K giants
  - Broach H & K CaII emission, sometimes Halpha
  - Periods several 0.1mag
  - May be former EW close binary systems observed at later stage

Variability linked to magnetism

- α^2 Canum Venaticorum
  - Highly magnetic B8p-A7p MS stars
  - Abnormally strong Si, Sr, Cr, and rare earths: vary with rotation phase
  - Variability 0.01-0.1 mag in V-band, periods 0.5-160+ days
- SX Ari hotter than α^2 CVn
  - B9p – B0p MS stars
  - Variable intensity He I and Si III lines
  - Periods around 1d, amplitudes about 0.1 mag in V-band

Magnetic Doppler Imaging in 4 Stokes parameters: α^2Canum Venaticorum (Kochukhov & Wade 2010)

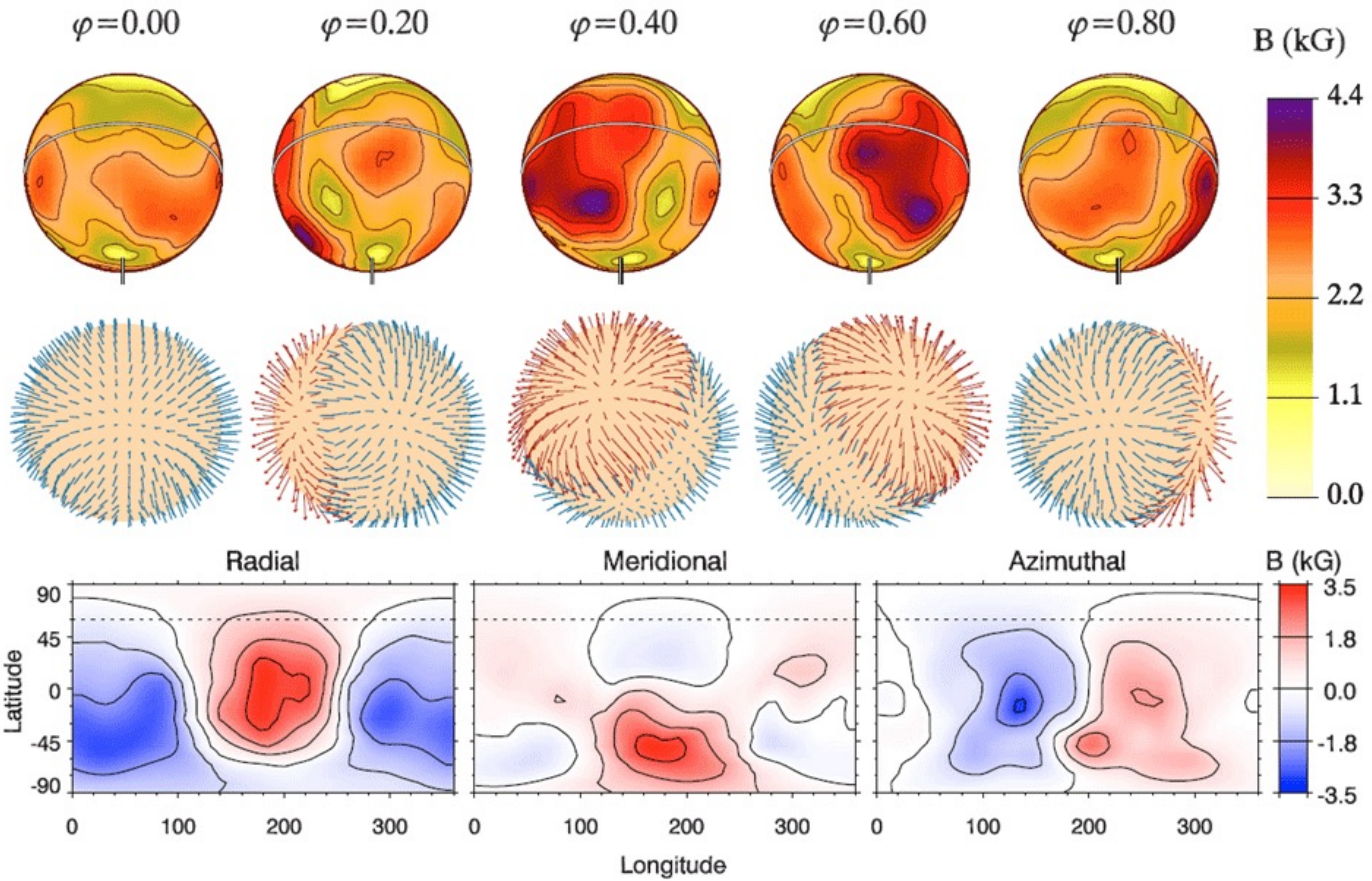

ζ Andromedae

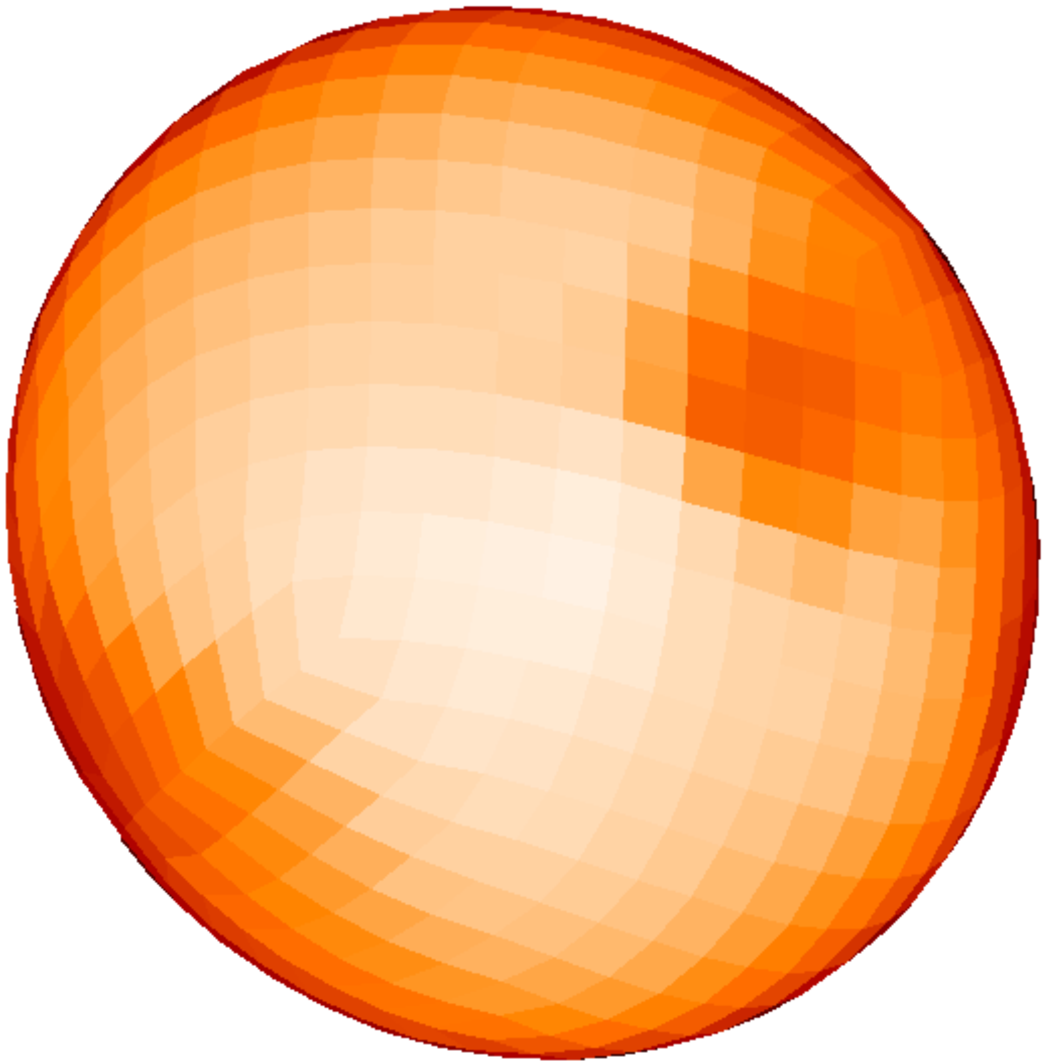

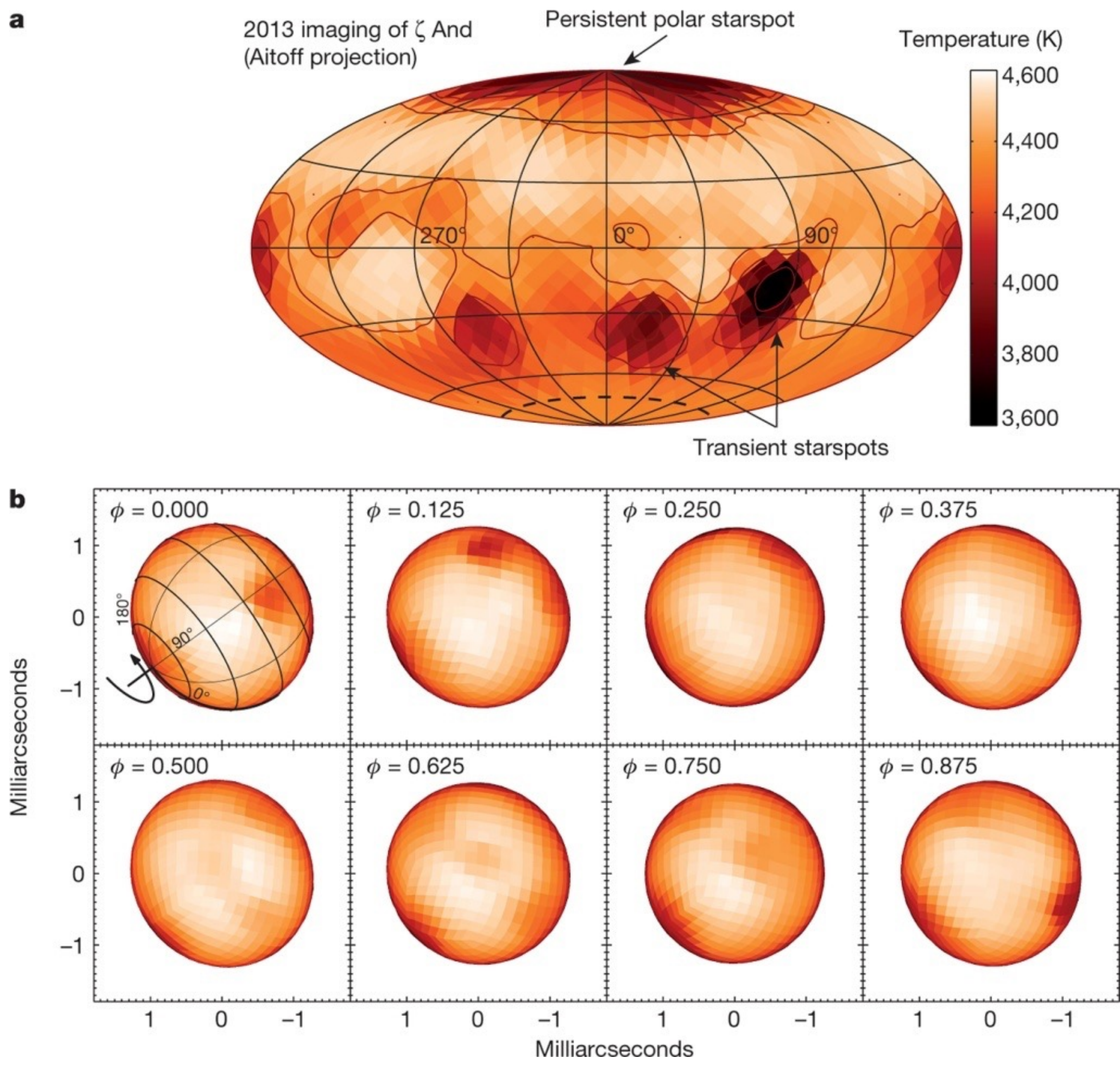

[Roettenbacher et al. (2016)]

Part II

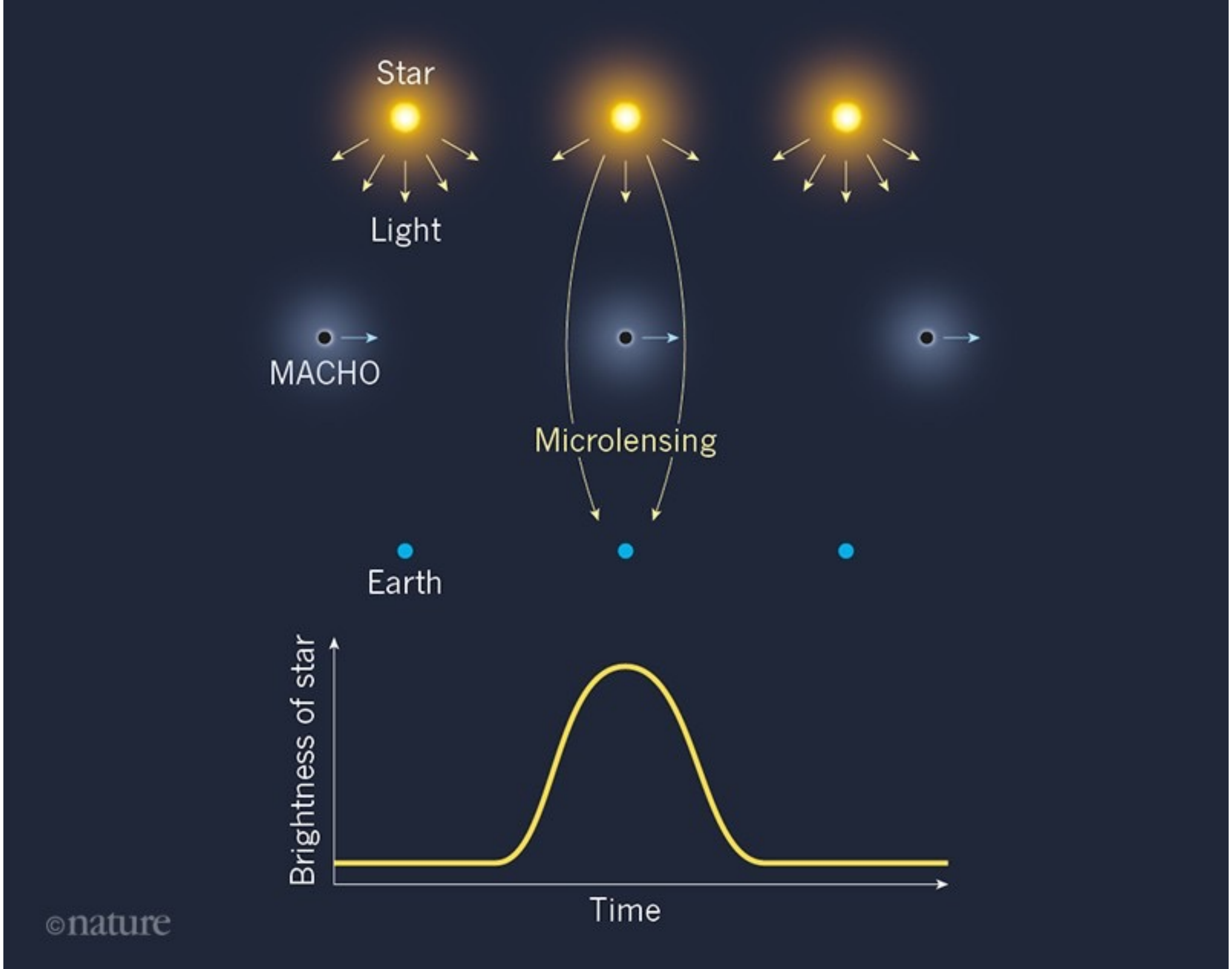
Star
Light
MACHO
Microlensing
Earth
Brightness of star
Time
©nature

Microlensing surveys

- Dense fields: LMC, SMC, Bulge
- First detection in 1990s by [Alcock et al. (1993)]
- Massive Compact Halo Objects: a candidate for dark matter?
- Too few events towards LMC to explain DM: [Wyrzykowski et al. 2011]
- If MW halo: low mass stars/NS, but origin more likely in LMC itself

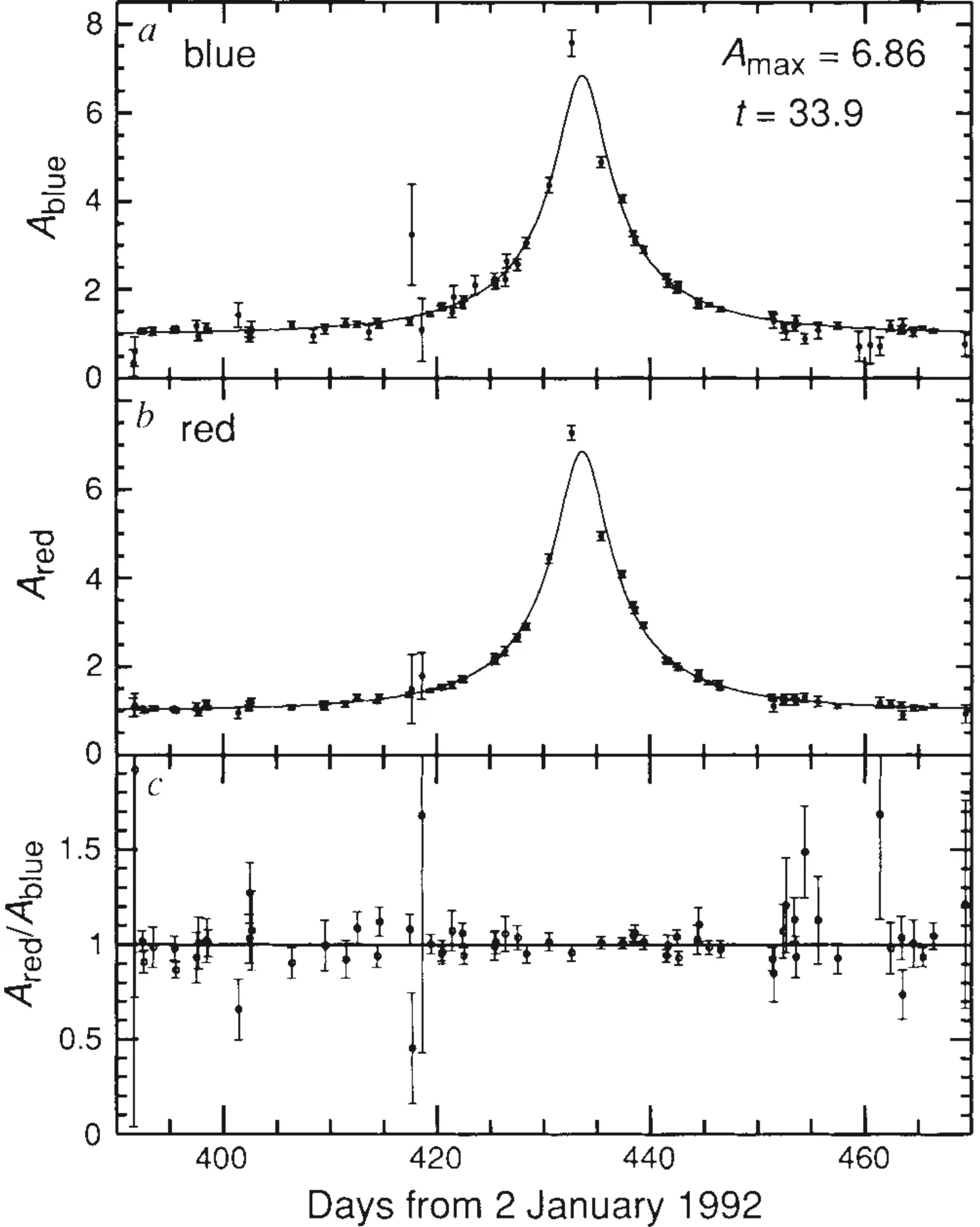

Tsapras (2018)

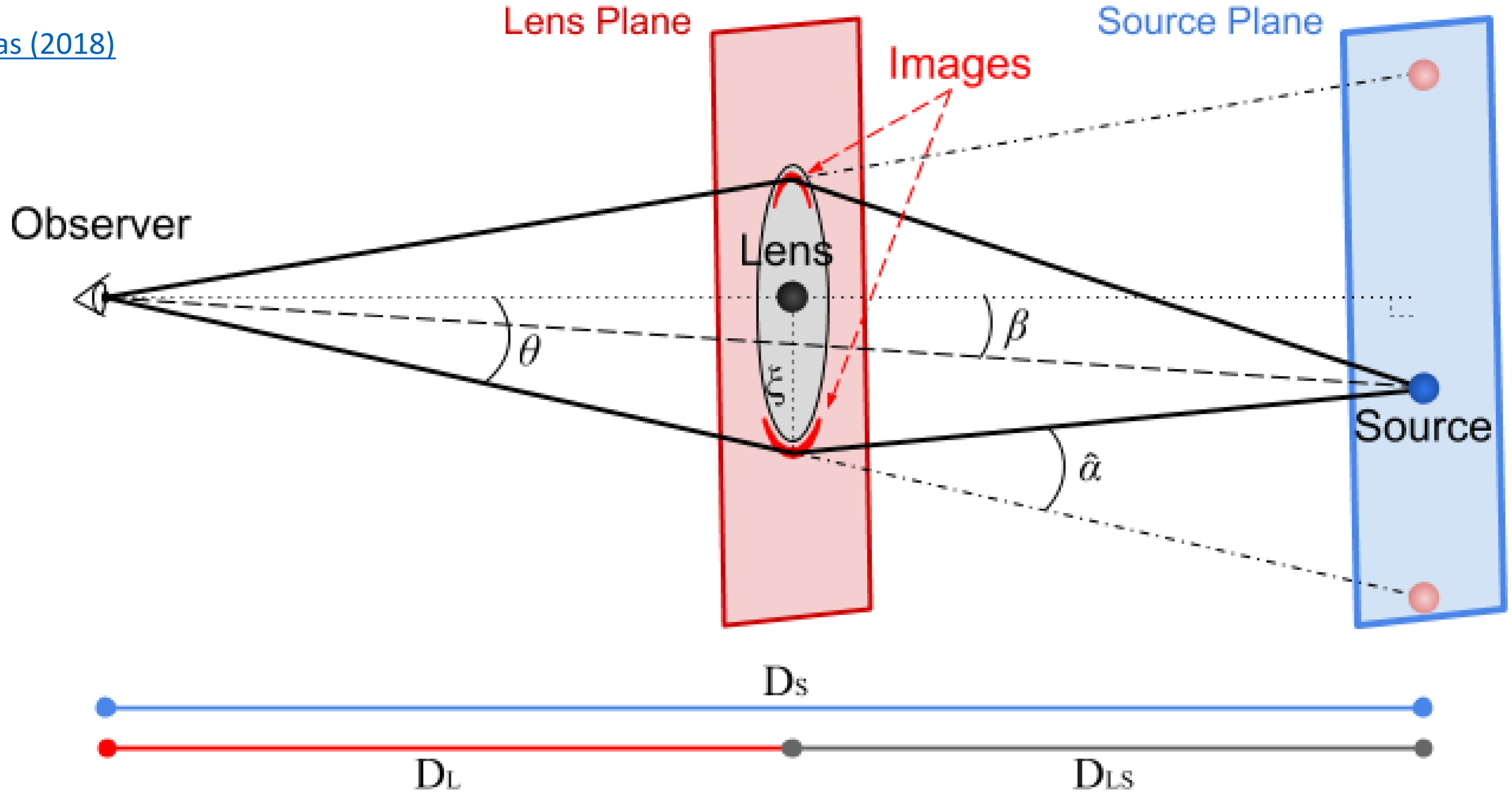

Figure 2
The geometry of a single lens microlensing event. Light rays originating from a source star are deflected near the lens. As a result, the observer does not perceive the light of the source itself, but instead measures the combined contribution of two distorted images of the source. The distances from the observer to the lens and the source are DL and DS, respectively. The distance between lens and source is DLS. β is the angular position of the unlensed source, α denotes the deflection angle and θ is the angular position of one of the images. The red and blue rectangles represent the parallel lens and source planes at DL and DS, respectively, which are perpendicular to the observer-lens axis (dotted).

Einstein (1936)

$$t_E = \theta_E / \mu_{rel}$$

$$\theta_E = \sqrt{\frac{4GM}{c^2} \frac{D_{LS}}{D_S D_L}}$$

$$M_L = \frac{\theta_E}{\kappa \pi_E}$$

$$\kappa \equiv \frac{4G}{c^2 au} = 8.144\, mas/M_\odot$$

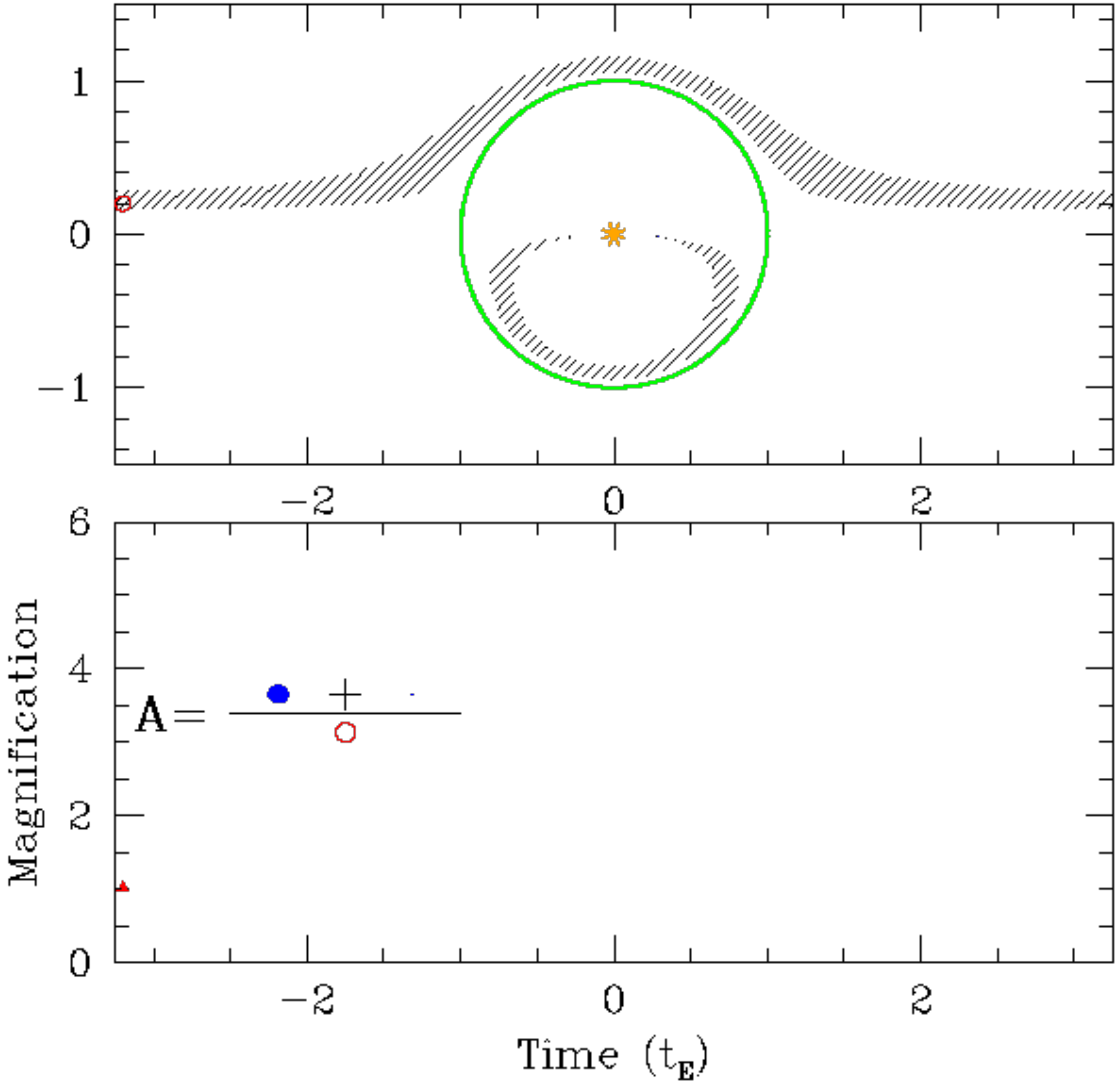

Tsapras (2018)

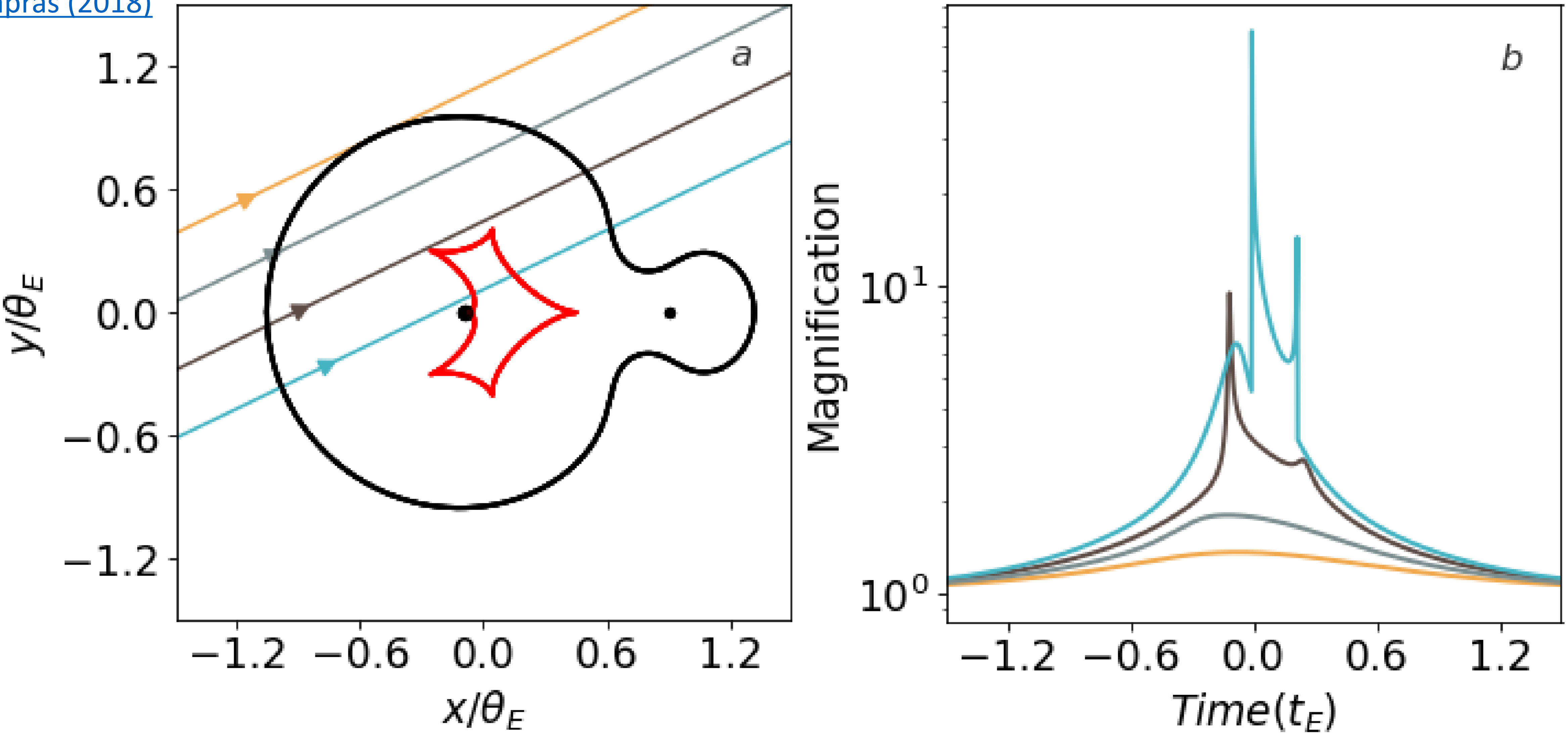

Figure 5

(a) Critical curves (black) and caustics (red) of a binary lens with s = 1, q = 0.1, assuming a point source. The origin is the center of mass of the system. When the lens is composed of two massive objects, the images of the source generated by the lensing effect are no longer two, but either three of five, depending on the location of the source relative to the caustics. For each of the four source trajectories considered, two new images get created or destroyed whenever the source crosses the caustic, producing the sudden 'jumps' in magnification seen in panel b. The positions of the two lensing masses are marked by the black dots and the x and y-axes mark distances on the lens plane in units of θE; (b) Corresponding light curves for each of the trajectories shown in panel a. Note the absence of sudden 'jumps' in magnification for the trajectories shown in orange and gray, where the source remains far from the caustics at all times.

Binary lenses

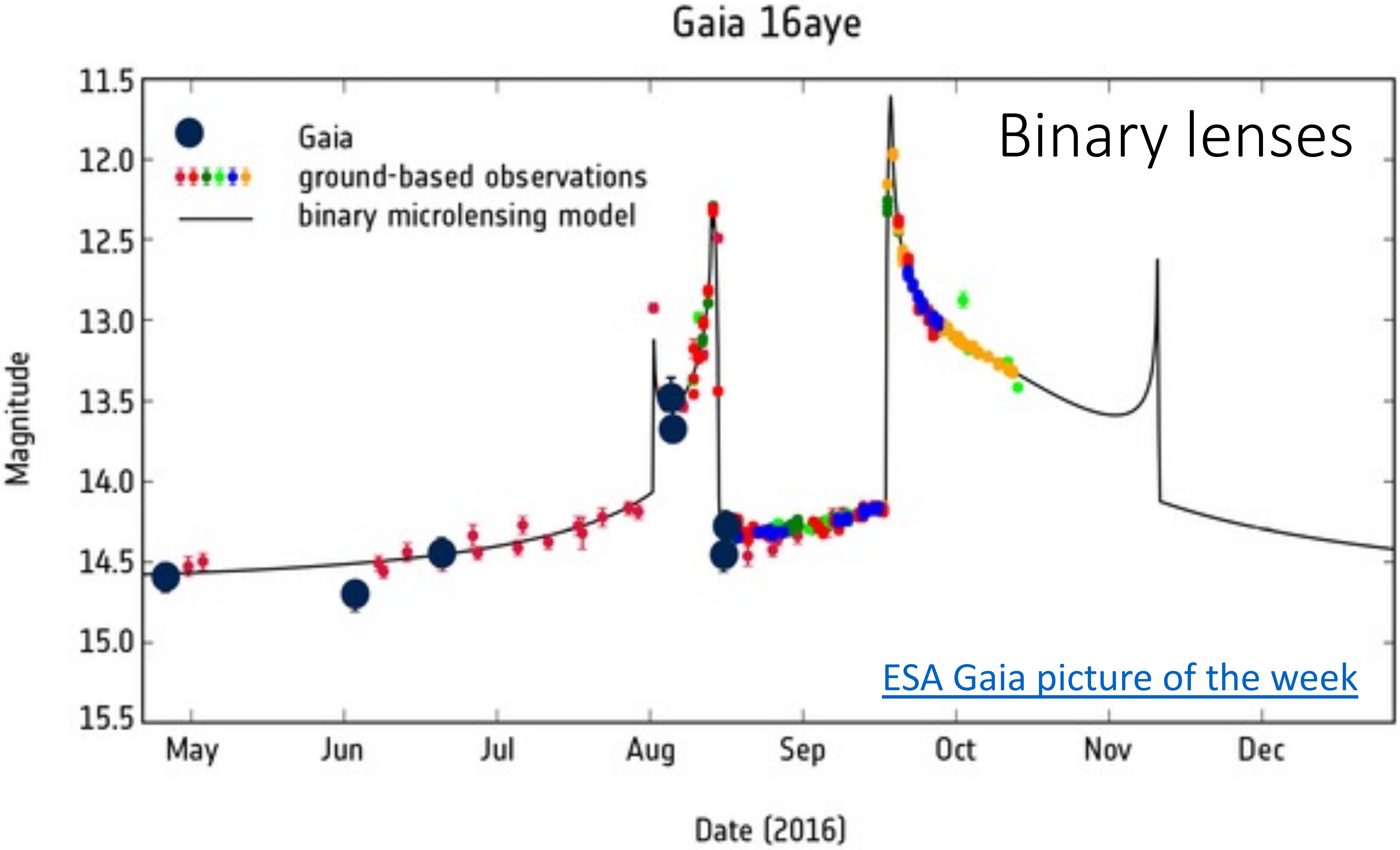

[ESA Gaia picture of the week]

Extrasolar planet detected by gravitational microlensing

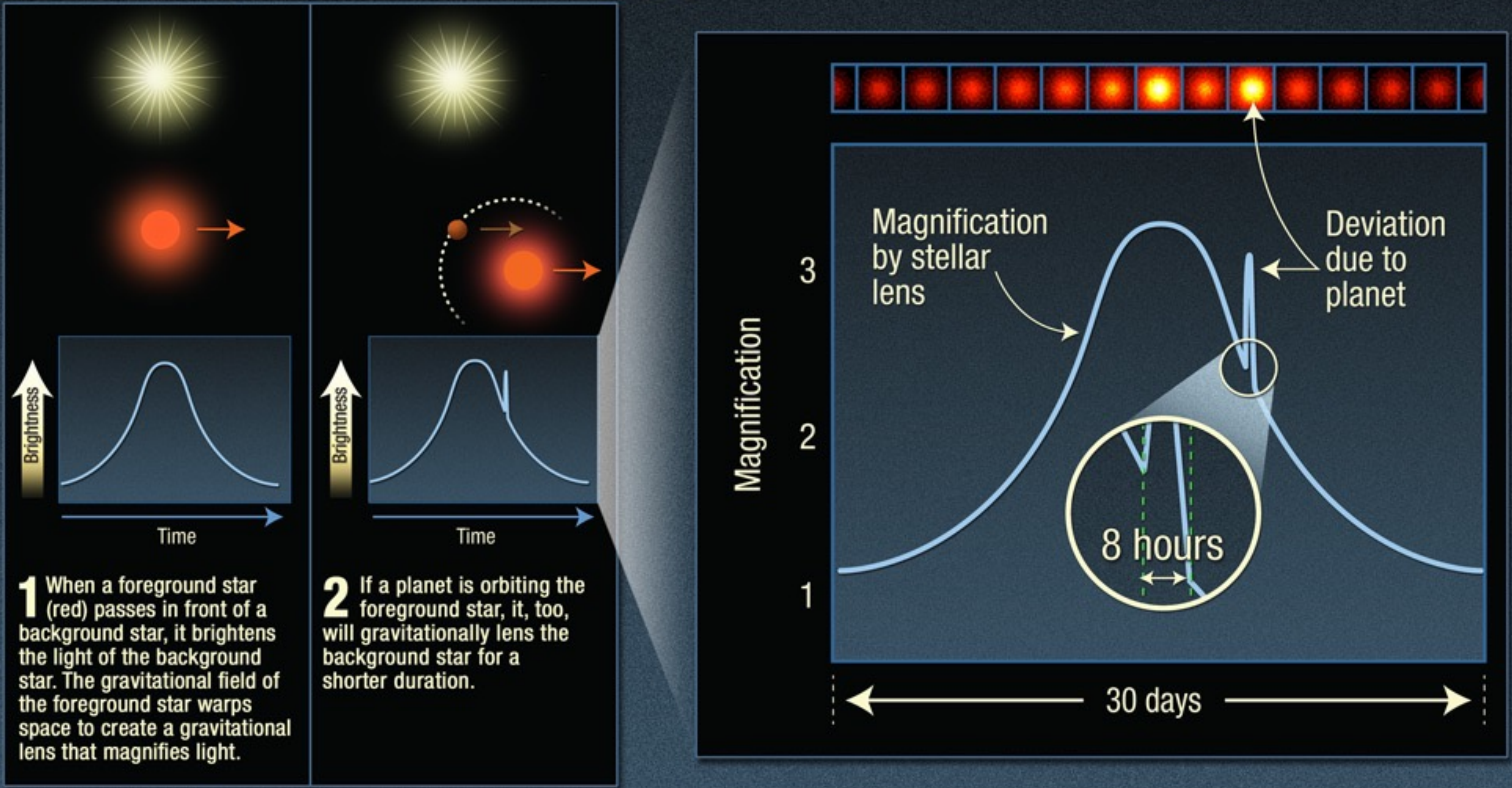

π_E : microlens parallax

Refsdal 1966; Gould 1992, 2000, 2004

- Need baseline to observe microlensing event at different times
- Orbital : Use Earth-Sun orbit ($t_E \geq yr/2\pi$)
- Terrestrial : different ground stations
- Satellite : ground + satellite baselines

$$t_E = \theta_E/\mu_{rel}$$

$$M_L = \frac{\theta_E}{\kappa\pi_E}$$

$$D_L = \frac{au}{\pi_{rel} + \pi_S}$$

$$\pi_{rel} = \pi_E\theta_E$$

$$\pi_S = au/D_S$$

$$\kappa \equiv \frac{4G}{c^2 au} = 8.144\, mas/M_\odot$$

Finding Planets With Microlensing

Astronomers use a technique called microlensing to find distant planets in the heart of our galaxy, up to tens of thousands of light-years away. This infographic illustrates how NASA's Spitzer Space Telescope, from its perch in space, helps nail down the distance to those planets.

A microlensing event occurs when a faint star passes in front of a distant, more visible star. The gravity of the foreground star acts like a magnifying glass to brighten the distant star. If a planet is present around the foreground star, its own gravity distorts the lens effect, causing a brief dip in the magnification.

The great distance between Earth and Spitzer helps astronomers determine the distance to the lensing planetary system. Spitzer can see lensing events before or after telescopes on Earth, and this timing offset reveals the distance to the system.

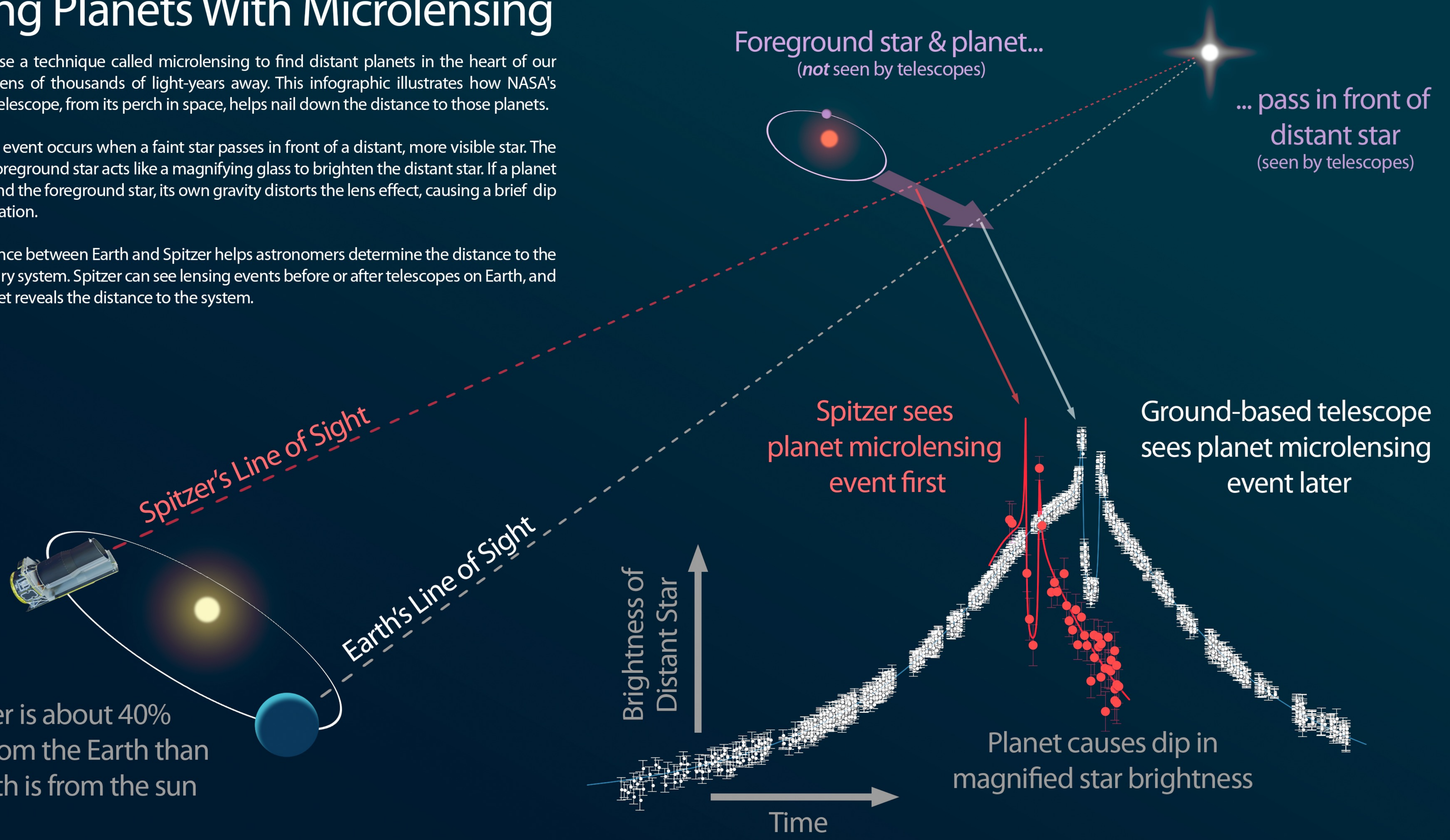

Microlensing parallax

Zang et al. (2020)

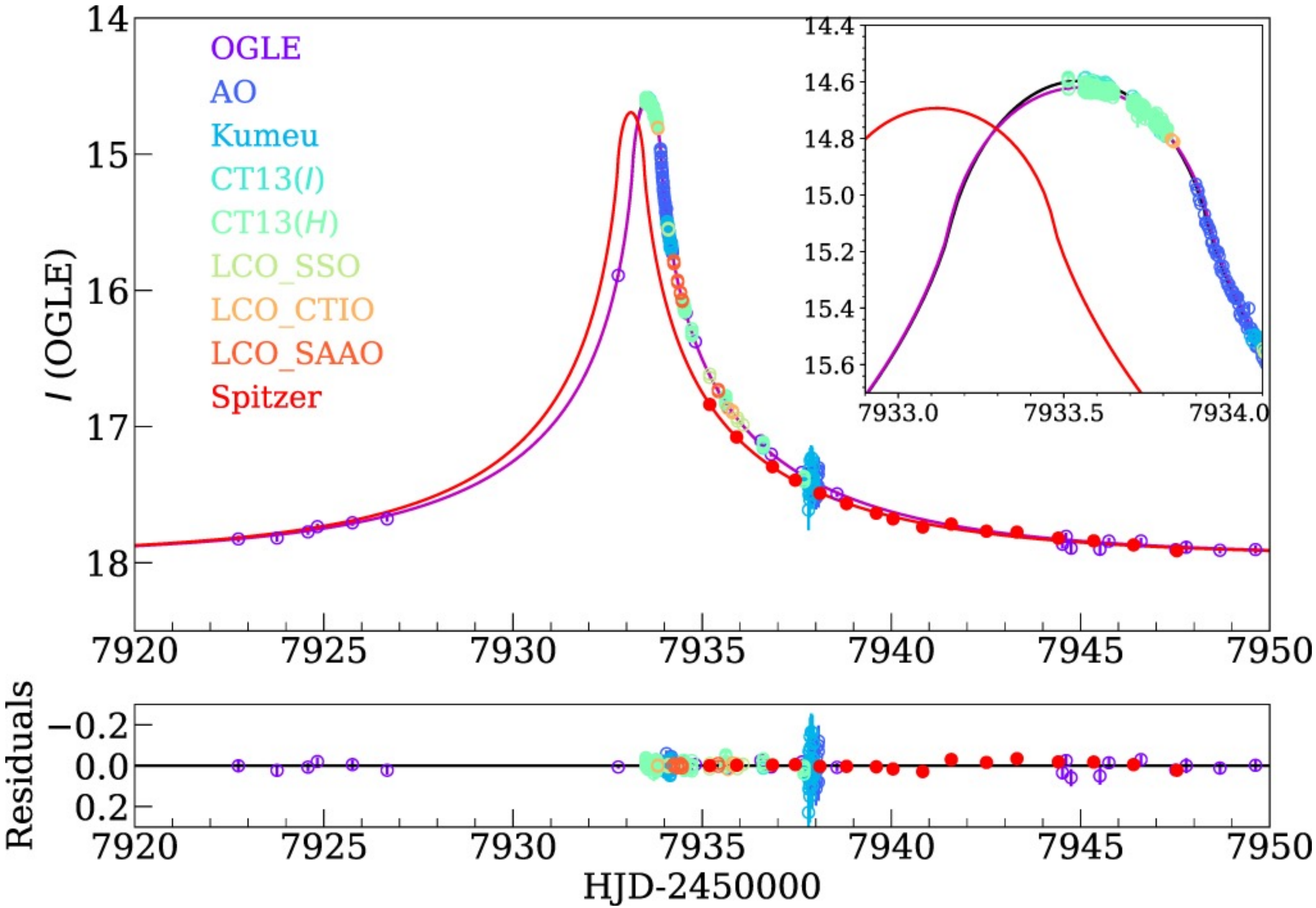

A resolved microlens!

Dong et al. (2019)

- Uses VLTI/GRAVITY
- $\theta_E = 1.87 \pm 0.03$ mas
- $\Delta\theta_{-,+} = 3.78 \pm 0.05$ mas
- Bright source K $\lesssim 10.5$
- Combining θ_E with π_E (Gaia) would yield M_L
- Rare falsification of Einstein: that "the luminous circle cannot be distinguished" from a star